MODELLING ARCTIC OCEANOGRAPHIC CONNECTIVITY

MAY 2021

ARCTIC COUNCIL

PAME

Protection of the Arctic Marine Environment

MODELLING ARCTIC OCEANOGRAPHIC CONNECTIVITY

TO FURTHER DEVELOP PAME'S MPA TOOLBOX

MAY 2021

Project leads

- Dr Jessica Nilsson (jessica.nilsson@havochvatten.se), Swedish Agency for Marine and Water Management
- Prof. Per Jonsson (p.r.jonsson@telia.com) and Prof. Göran Broström (goran.brostrom@marine.gu.se), Department of Marine Sciences, University of Gothenburg, Sweden
- Other contributing partners
- Prof. Martin Nilsson Jacobi (mjacobi@chalmers.se), Chalmers University of Technology, Sweden

We would like to extend our sincere appreciation to all the experts who have contributed with wise comments and useful suggestions.

Swedish Agency for Marine and Water Management

PAME
Protection of the Arctic Marine Environment

ARCTIC COUNCIL

Table of Contents

I. EXECUTIVE SUMMARY

Seascape connectivity in the Arctic Ocean of species with passive dispersal is explored using two oceanographic circulation models (Arctic4 and TOPAZ) combined with Lagrangian particle tracking, simulating drifting eggs and larvae of invertebrates and fish. Particles were released in the Arctic shelf area (depth ≤ 500 m) from 40893 model grid cells. A literature survey of invertebrate and fish larvae guided the selection of parameters for the particle tracking model, although little is still known about dispersal characteristics in the Arctic Ocean. In the near absence of information about dispersal traits for most species, the simulations of particle dispersal covered a wide range of combinations of drift depths (0-150 m) and pelagic larval durations (PLD, 5-90 days). The particle tracking simulations were repeated for the years 2007-2016, and between 1991-2015 for surface water. The core result is a database of a large number of connectivity matrices specifying the probability of dispersal between all 40893 seascape locations and for all combinations of spawning time (each month), depth of dispersal and PLD. From the connectivity matrix a range of metrics may be calculated to estimate different aspects of seascape connectivity, e.g. dispersal distance from any location, source and sink dynamics, local retention and network properties for Marine Protected Areas (MPAs), and identification of partial dispersal barriers.

Modelled dispersal distance showed a significant increase with PLD, while depth had a smaller effect, although the geographic location greatly influenced dispersal distance. We also demonstrate how source and sink analyses can be used to estimate the effect of MPAs on ambient areas, e.g. as source of larvae, but also how MPAs may act as a sink for contaminants and other distant pressures. Self-recruitment within MPAs may be essential for the persistence of protected populations. Using the connectivity matrix, it is shown how self-recruitment based on local retention of larvae depends on drift depth and PLD, and also on the particular location and size of MPAs.

From the connectivity matrix partial dispersal barriers in the seascape may be identified and visualised. A preliminary analysis shows how the shelf area can be subdivided into areas separated by dispersal barriers and how these dynamically change with larval dispersal traits.

Modelled connectivity metrics show seasonal changes probably caused by the change in sea ice cover. It is also interesting to note that a preliminary analysis shows some putative trends in seascape connectivity between 1991-2015 mainly during the warm season with a generally negative trend in local retention in MPAs, although there seems to be regional differences. These trends in seascape connectivity may be further amplified assuming projected climate change. Finally, future research using empirical methods, e.g. genetic markers, will be valuable in validation of modelled connectivity and dispersal barriers.

II. OBJECTIVES

This report is aimed as a working document and is a contribution to the protection of the Arctic marine and coastal environments from the Swedish delegation within the working group 'Protection of the Arctic Marine Environment (PAME)'. The overall aims are to contribute to the PAME's MPA toolbox by:

- mapping potential **connectivity** among populations of key marine species in the Arctic region using biophysical modelling to inform the positioning and nature of conservation measures deployed in a network of MPA
- describing dispersal distance within the Arctic Ocean, which may be used to infer the **minimum size** of Marine Protected Areas (MPAs) for sufficient self-recruitment
- identifying **sources and sinks** for MPAs and other valuable areas, e.g. fish spawning grounds and juvenile nursery areas
- identifying major **barriers** to dispersal and gene flow

III. BACKGROUND

PROTECTION OF THE ARCTIC MARINE ENVIRONMENT

The Arctic Council working group PAME (Protection of the Arctic Marine Environment) aims to suggest and support actions for the protection of the Arctic marine environment. Ongoing climate change is already facilitating increased access to the Arctic region, leading to greater use and new economic opportunities, but also bringing potential threats to the Arctic marine and coastal environments. These changes require more integrated approaches to Arctic marine protection, including spatial planning of protection measures to ensure sustainable use of the Arctic environment.

Networks of Marine Protected Areas (MPAs) are now considered to be an effective instrument to mitigate extractive and local disturbance effects on harvested stocks, general biodiversity, and ecosystem services (Lester & Halpern 2008). Well designed and managed MPA networks can also improve local resilience to large-scale pressures like effects from climate change (Micheli et al. 2012). When selecting areas as MPAs, it is important to ensure that they are designed to have the capacity to protect target populations. As an example, one design criteria can be to create MPAs that provide "ecologically coherent" networks that ensure dispersal, migration and genetic exchange of individuals between relevant sites improving resilience to disturbance or damage caused by natural and anthropogenic factors (OSPAR 2013, HELCOM 2016, Jonsson et al. 2020). Key aspects of this design are the size of individual MPAs and how they are connected through dispersal to the ambient environment.

Ecological connectivity is essential for the survival and migration of species and for evolutionary adaptation of populations. The increasing habitat fragmentation calls for management and conservation actions, e.g. MPAs, that promote ecological connectivity (PAME 2015). Maintaining source-sink dynamics and ensure adaptation processes in ecosystems is necessary to combat the decline in biodiversity and to build resilience especially in view of the ongoing climate change. Organisms with long-distance dispersal of eggs and larvae may require very large MPAs, or a network of smaller MPAs that can exchange dispersal stages within the network, or with surrounding areas.

BIOPHYSICAL MODELLING OF DISPERSAL

More than 70% of marine invertebrates and fish disperse with large numbers of microscopic eggs and larvae that may drift for days to months with the ocean currents. Although larvae, for the most part, disperse passively, they may nonetheless influence their transport through vertical migration to different depths with different current patterns. Thus, it is very difficult to make direct observations of dispersal in the field, although genetic methods can be used to coarsely infer dispersal (e.g. Jorde et al. 2015, Jahnke et al. 2018). *Biophysical modelling* is increasingly used to estimate dispersal in the seascape (Cowen & Sponaugle 2009, van Sebille et al. 2018). Here a physical ocean circulation model is used to realistically simulate how the three-dimensional (3-D) circulation field, as well as temperature, salinity and ice, vary in space and time. The oceanographic model of sea

More than 70% of marine invertebrates and fish disperse with large numbers of microscopic eggs and larvae that may drift for days to months with the ocean currents.

currents is then combined with a biological model that defines the traits for a particular species (or dispersal strategy), such as spawning time, drift duration of the larvae (pelagic larval duration, PLD), and any larval behaviour, e.g. vertical migration or ontogenetic shifts in drift depth. Such a biophysical model can simulate the transport paths of virtual larvae allowing the "release" of many millions of virtual larvae at many spawning sites (sources), and includes temporal variability in currents on scales from days to years. The biophysical modelling of larval dispersal presented here is mainly relevant for organisms with sedentary adults where connectivity largely depends on physical water transport of larvae or other propagules. For dispersal and connectivity of migrating fish, marine mammals and birds other methods have to be used, e.g. marking and tracking.

The model results of each larval dispersal simulations are summarized in a connectivity matrix, where each element gives the probability of dispersal from site A to site B (Jonsson et al. 2020). For the area included in the model, the connectivity matrix fully describes connectivity for the target species (or the dispersal strategy) in the seascape. A major advantage with a database of connectivity matrices based on combinations of trait values as spawning time, drift depth and PLD, is that these matrices can be combined and averaged to represent many different species or survival strategies (Jonsson et al. 2020).

IV. METHODS

REVIEW OF PUBLISHED INFORMATION ON LARVAL DISPERSAL TRAITS IN THE ARCTIC OCEAN

A starting point was to review studies from the Arctic Ocean that report data on traits for larvae of marine invertebrates and fish that may affect dispersal patterns. The focus is on the dispersal of planktonic larvae that largely drift with the ocean currents. Traits assumed to be most influential on dispersal are spawning season, the amount of time larvae drift in the water column (pelagic larval duration, PLD), and the depths at which larvae are drifting (Corell et al. 2012). There is also the possible occurrence of more complex, behavioural vertical migration schemes. However, considering the sparse literature, it is not surprising that this information is lacking at present. Thus, we will only consider relatively simple traits in this pre-study.

A number of search strings were used to query the Web of Science database (Clarivate Analytics), including 'marine', 'larva*', 'arctic', 'polar', 'dispersal', and 'connectivity'. We also received some input from Dr. Tom Christensen at the Conservation of Arctic Flora and Fauna (CAFF) and Dr. Jørgen Hansen at the University of Aarhus. This search resulted in only a few publications with data on larval traits, and a handful of species. Despite the paucity of relevant publications, the data from these studies could guide the selection of major spawning times and dominant depth intervals for larval dispersal of selected species as simulated with the biophysical model.

OCEANOGRAPHIC CIRCULATION MODEL

We have used two existing oceanographic models, the Arctic4 and the TOPAZ, which include the Arctic Ocean and North Atlantic in their domains. *TOPAZ* (e.g., https://os.copernicus.org/articles/8/633/2012/) has been developed at the Nansen

Centre in Bergen over a number of years, and is currently, its operational model is run weekly by the Norwegian Meteorological Institute (MET). It is also run in a re-analysis mode by the Nansen Centre. TOPAZ is the main operational, and re-analysis model for the Arctic Ocean in the marine Copernicus data portal (https://marine.copernicus.eu). TOPAZ has stereographic projection with 12.5 km horizontal resolution and has 28 vertical (isopycnal) layers. Results for the 5 m level has been used for the present study (the TOPAZ products in the Copernicus data portal are interpolated to 12 unevenly (Levitus) spaced vertical levels: 5, 30, 50, 100, 200, 400, 700, 1000, 1500, 2000, 2500 and 3000 m), although a new re-analysis with a higher vertical resolution output at Copernicus data portal will be available in the near future. We here used daily averaged velocity fields from 1991 to 2015.

The Arctic4 model has a horizontal resolution of 4 km and 32 vertical sigma-coordinate layer (i.e. the layers follow the bottom topography and vertical resolution is thus higher at shallower regions) and was developed by MET and AkvaPlan-Niva with the aim to become an operational model, however, this plan was abandoned with the introduction of TOPAZ as the main operational model for the Arctic Ocean. Arctic4 has been run for more than 10 years by researchers at MET and AkvaPlan-Niva but has not gone through the same extensive validation as is typical for operational models. In this study, daily averaged velocity fields between 2007-2016 were used.

All available velocity fields, along with associated information on temperature, salinity and ice, have been downloaded and pre-processed for use in a Lagrangian particle tracking model that simulates dispersal trajectories. The pre-processing includes extracting data north of 65^{o}N and saving as single precision in Matlab native format for rapid reading; Arctic 4 data were interpolated to prescribed depth levels. Mean drift patterns as well as interannual variability in drift patterns have been targeted. It should be noted that while other oceanographic model setups with higher resolution exist, results are not easily available for long-term analyses (i.e. may require new production of velocity fields from the hydrodynamical model). Furthermore, not all models use data assimilation, such as e.g. TOPAZ does.

PARTICLE TRACKING MODEL

A Lagrangian particle-tracking model uses available model prediction of ocean currents to move particles in the ocean (van Sebille et al. 2018). An in-house particle-tracking model was used and developed in MATLAB® (MathWorks Inc.), but a number of similar models exist in the literature and are downloadable from the web, although different programming languages are used. For the present study, we used a time step of 1 hour, since only daily averaged velocity fields were available. In the absence of field information about larval vertical behaviour in the Arctic Ocean, we only considered horizontal drift at specified depth intervals during the whole PLD, although we simulated drift in a number of specified depths (see below). Furthermore, we did not use any horizontal dispersion (or random walk) of particles, as is frequently used to mimic unresolved turbulent processes. This is because the particle fields (or velocity fields) are very dispersive in themselves (see e.g. Fig. 6) and we believed including “extra” dispersion was unnecessary (as verified by preliminary tests).

A critical decision for the particle tracking simulations is how many release sites to consider, the number of release time points, and how many particles to release on each occasion. To provide non-trivial results for the last case would require

numerical dispersion to be included. The ideal situation is to include all of the model grid cells that overlap with the target habitat as sources of particles in the Lagrangian tracking model. As a compromise between conservation interests and practical limits of numerical computation it was decided to include all areas shallower than 500 m in the TOPAZ model bathymetry above the arctic circle. With a 12 km grid, this area resulted in 40893 release points in the model domain, shown in Fig. 1. From each release point, one particle ('virtual larva') was released every day and tracked through its PLD. Daily releases were repeated all-year-round for at least 10 years. For the Arctic4 model, particles were released between 2007-2016, and for the TOPAZ model, particles were released between 1991-2015. Based on velocity fields from the Arctic4 model particles were released and constrained to the following depths: 0, 5, 10, 15, 20, 30, 50, 70, 100 and 150 m depth. Velocity fields from the TOPAZ model were only used to track particles in the surface layer (0-5 m). The positions of each particle were saved daily, but in subsequent analyses we only considered drift after 5, 10, 15, 30, 45, 60 and 90 days.

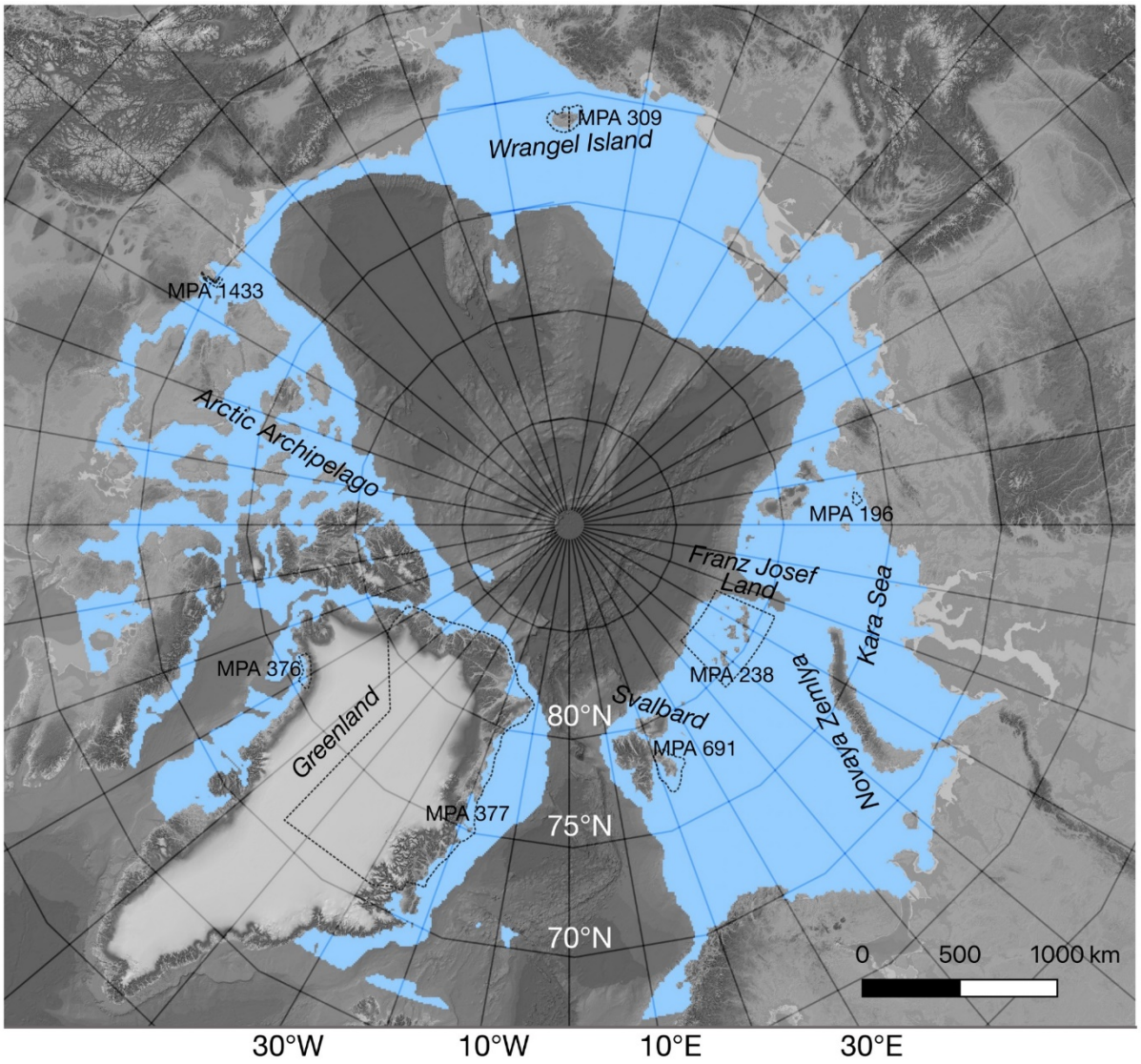

Fig. 1. The Arctic Ocean with the biophysical model domain (depth ≤ 500 m) shown in blue including 40893 model grid cells. Also shown are the selected Marine protected Areas: MPA 196 – Bolshoy, MPA 238 – Franz Josef Land, MPA 309 - Wrangel Island, MPA 376 – Melville Bay, MPA 377 – East Greenland, MPA 691 – Svalbard, MPA 1433 - Anguniaqvia.

The dispersal trajectory data produced by the Lagrangian particle-tracking model are extensive (ca. 10^{10} positions) and are summarized into mean connectivity matrices specifying potential dispersal probability (Watson et al. 2010) between all 40893 model grid cells. Each connectivity matrix consists of 40893 rows and columns with each element specifying the probability to disperse from grid cell *j* (column *j*) to grid cell *i* (row *i*). Figure 2 schematically shows the construction of the connectivity matrix. For the connectivity matrices, we averaged dispersal probability for each month and across a 10-year and 25-year period for the Arctic4 and the TOPAZ models, respectively.

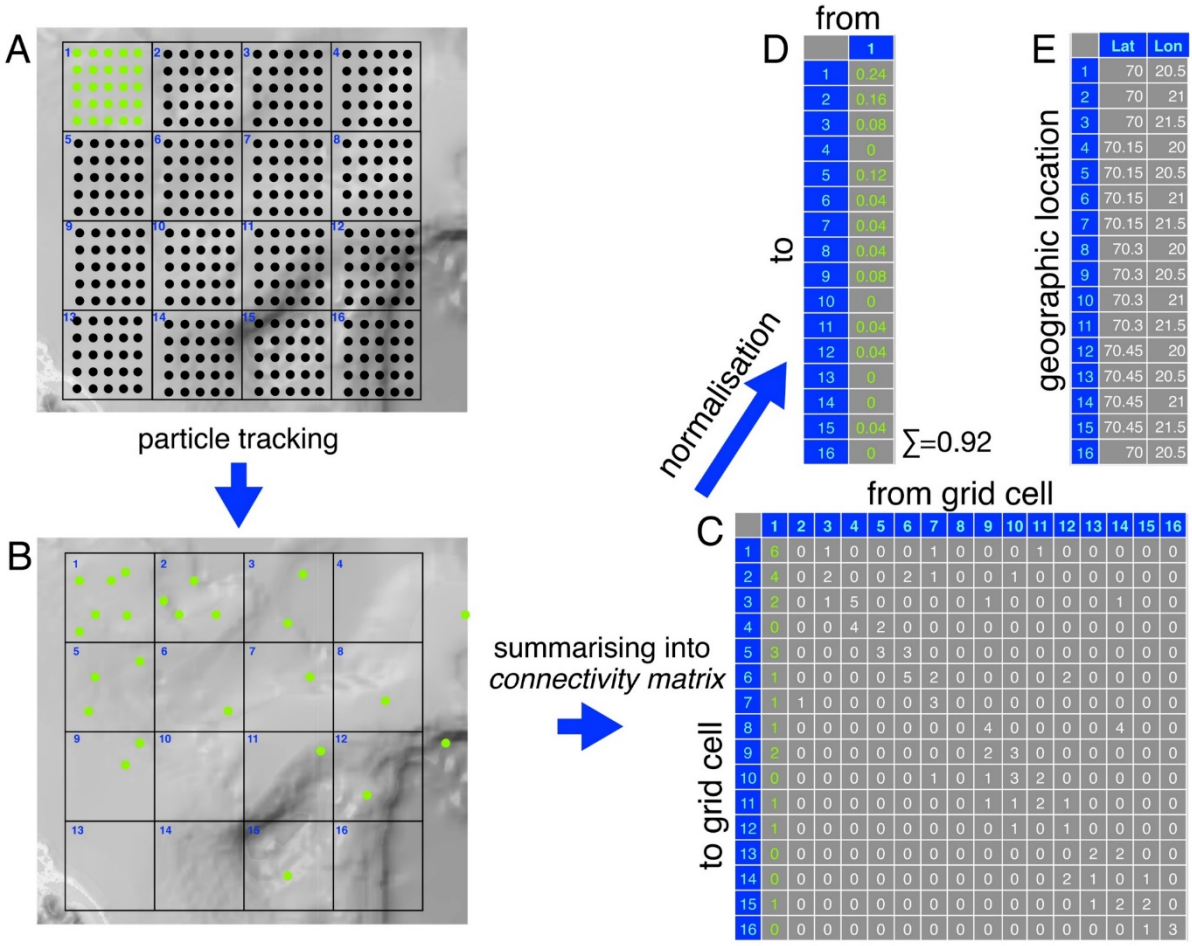

Fig. 2. Schematic drawing showing the particle tracking procedure and the construction of the connectivity matrix. (A) Each grid cell in the model domain is seeded within some season and depth with a number of particles, in this example 25 particles. Note that each grid cell has an identification number, here from 1 to 16. (B) When the seeded particles have been transported by the ocean circulation for a specified PLD, the resulting positions are recorded. This panel shows the positions of the particles seeded in grid cell No 1 (the green circles). (C) The result is summarised into a connectivity matrix, where each element indicates how many particles seeded in column j ended up in row i, where j and i are the identities of the source and sink grid cells, respectively. For the green particles seeded in grid cell 1, the results are filled into the rows of column 1, e.g. grid cell 9 received 2 particles from grid cell 1. (D) The numbers in the primary connectivity matrix are converted or normalised to probability by dividing by the number of particles seeded into each grid cell, in this case 25. Thus, the table in panel D shows the dispersal probability of dispersing from grid cell 1 to grid cells 1 to 16. (E) Also needed is the geographic location of each grid cell (latitude and longitude) where each row number corresponds to the grid cell number.

We further constructed separate connectivity matrices for the warm season (March-October) and the cold season (November-February). This division into two seasons was based on the literature review of larval abundance (Fig. 5) and the ice cover (National Snow and Ice Data Centre 2019). Separate connectivity matrices were constructed for the drift depths of 0, 10, 15, 30, 50, 70, 100 and 150 m and for the PLDs of 5, 10, 15, 30, 45, 60 and 90 days resulting in a total of 56 matrices for each season. In addition, 7 connectivity matrices per season were constructed for the surface drift based on the TOPAZ model. Each connectivity matrix may be viewed as the dispersal pattern for a specific combination of dispersal traits in terms of spawning season, drift depth and PLD. It is also possible to generate more complex dispersal strategies by combining several connectivity matrices (e.g. Jonsson et al. 2016). An example of a connectivity matrix produced within the project is shown in Fig. 3 with all elements greater than zero (i.e. connectivity between grid cells) indicated in blue.

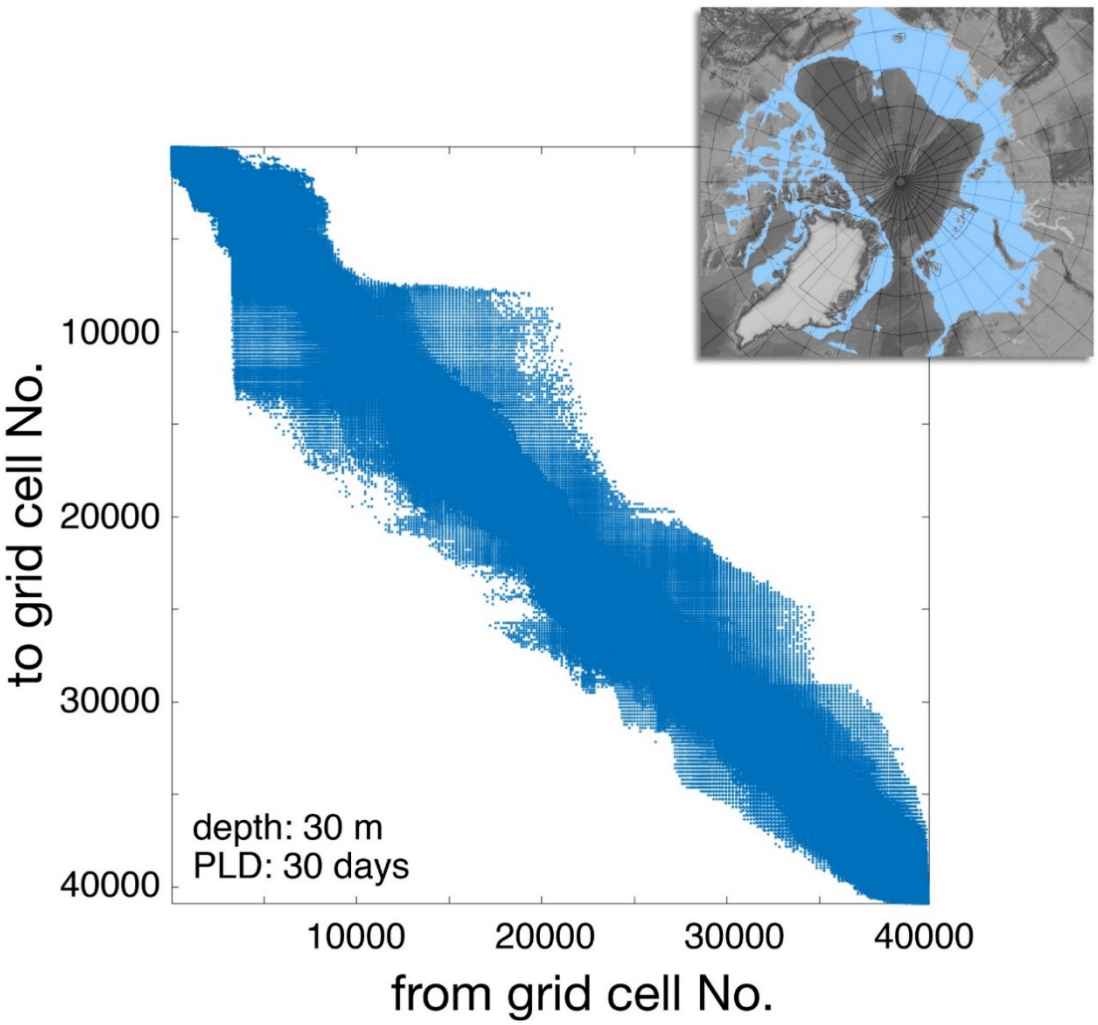

Fig. 3. A visualisation of a connectivity matrix for the whole model domain of 40893 grid cells (inset). The blue elements indicate all non-zero dispersal probabilities between grid cells. Note that the connectivity matrix is read as the probability of dispersal from column j to row i. The matrix is sparse and we only save non-zero data to save space.

CALCULATION OF DISPERSAL DISTANCE

For each model grid cell that is included in the Lagrangian trajectory model (Fig. 1), the weighted mean of local dispersal distance was calculated based on the dispersal probability and the Euclidean distance between grid cells specified by the connectivity matrices. The weighted mean dispersal distance ($\bar{l}$) from each source grid cell i was estimated as:

$$\bar{l}_i = \sum_i^N C_{ij} \cdot D_{ij} \qquad \text{Eq. 1}$$

where C_{ij} is a vector with connectivity from grid cell i to all other N grid cells, and D_{ij} is a vector of geographic distance from grid cell i to all other grid cells. The mean dispersal distance was calculated for a selection of combinations between drift depth and PLD (see Results). Local dispersal distance can be important when designing MPAs and determining the adequate size that can allow sufficient self-recruitment to ensure population persistence (Jonsson et al. 2020).

IDENTIFICATION OF SOURCES AND SINKS

From the connectivity matrix, it is possible to identify the sources and sinks of a particular area (e.g. an MPA, a spawning ground or a nursery area). Sources may include a tracer of some pressure (e.g. contaminants or suspended matter) or biological propagules like seeds, eggs or larvae. The areas receiving propagules from an MPA acting as a source are found by summing columns representing locations where the MPA overlaps with the model grid cells (Fig. 4). Areas outside the MPA that act as sources for a particular MPA are instead found by summing the rows representing locations where the MPA overlaps with the model grid cells. As an example, source and sink areas were identified for seven selected areas (for illustration), with some marine extension, included in CAFF protected areas (CAFF 2013). The selected areas were ID 196-Bolshoy, ID238-Franz Josef Land, ID309-Wrangel Island, ID376-Melville Bay, ID377-North-East Greenland, ID691-Svalbard, and ID1433-Anguniaqvia. Source and sink analyses were carried out for combinations of drift depth and PLD. This analysis assumes that an abiotic tracer or biological propagules maintain their position within specific depth intervals during transport. Many invertebrate and fish larvae show diurnal, circatidal or ontogenetic shifts in vertical position (e.g. Moksnes et al. 2014)

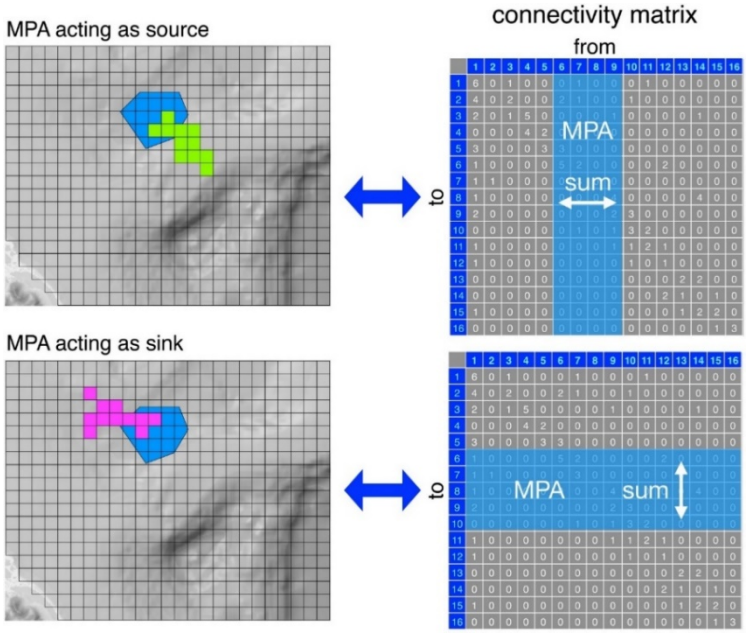

Fig. 4. Schematic drawing illustrating the identification of areas receiving propagules from an MPA (blue polygon), and areas providing propagules to the MPA. In the top left panel the MPA acts as a source to ambient areas (green grid cells). The green areas are found by first identifying the grid cell numbers matching the location of the MPA. The columns representing these grid cells are summed row-wise (blue columns) and normalised to the number of columns. The resulting non-zero elements represent the areas (green grid cells) receiving propagules from the MPA. Symmetrically, the pink areas providing propagules to the MPA in the bottom-left panel can be found by identifying the row numbers corresponding to the grid cells matching the MPA location (blue rows). Summing these rows column-wise produces a vector where the non-zero elements represent the pink areas acting as a source to the MPA.

CALCULATION OF LOCAL RETENTION FOR MPAS

For existing or planned MPAs, the connectivity matrix can be directly used to calculate the predicted local retention of larvae (i.e. the probability that larvae released within the MPA also end their trajectory within the same MPA). The elements in the connectivity matrix overlapping with each MPA were extracted and summed to obtain the estimated mean local retention ($\bar{r}$) for each MPA as:

$$\bar{r} = \sum_1^{n \cdot n} C_{MPA,MPA} \cdot 1/n \qquad \text{Eq. 2}$$

where $C_{\text{MPA, MPA}}$ is a sub-matrix with connectivity for the n grid cells located within the MPA. Local retention is a necessary condition for self-recruitment, but not the only consideration.

IDENTIFICATION OF DISPERSAL BARRIERS

Bathymetric features, habitat distribution and consistent circulation patterns may lead to dispersal barriers in the seascape with consequences for exchange of individuals and genes between sub-populations. A previously developed clustering method was employed to identify partial dispersal barriers from the constructed connectivity matrices (Nilsson Jacobi et al. 2012, Jonsson et al. 2020). This theoretical framework finds clusters as a signature of partially isolated sub-populations. Identification of subpopulations is formulated as a minimization problem with a tuneable penalty term that makes it possible to generate population subdivisions with varying degree of dispersal restrictions. Areas that have an internal connectivity above the dispersal restriction are colour-coded, and the transitions of colours indicate partial dispersal barriers. Barriers may differ among dispersal strategies and habitats. Strong barriers may indicate the presence of locally adapted sub-populations with unique genetic compositions. Also, relatively weak barriers may indicate limited exchange of individuals, which may not be sufficient for genetic differentiation but may call for separate management plans for harvested populations.

V. RESULTS

REVIEW OF PUBLISHED INFORMATION ON LARVAL DISPERSAL TRAITS IN THE ARCTIC OCEAN

The most commonly reported data are the occurrence of invertebrate and fish larvae over time in the water column, often with only broad taxonomic identification. It was also possible in many cases to infer the depth interval where larvae were caught, although only a few studies presented depth profiles. Few studies reported data on PLD, although PLD could in some cases be coarsely inferred from the occurrence over time in the water column.

Table A1 (see Appendix) shows extracted data from 10 publications. A coarse overview of the temporal occurrence of larvae in the water column is shown in Fig. 5, expressed as number of taxa found at different time periods. The blue line indicates the time of the year when larvae are first observed and the orange line represents when they disappear. It is clear that the majority of larvae disperse during the warmer half of the year, with peak abundances in May to August. This graph guided the subdivision of connectivity matrices into the two seasons "warm" (March-October) and "cold" (November-February).

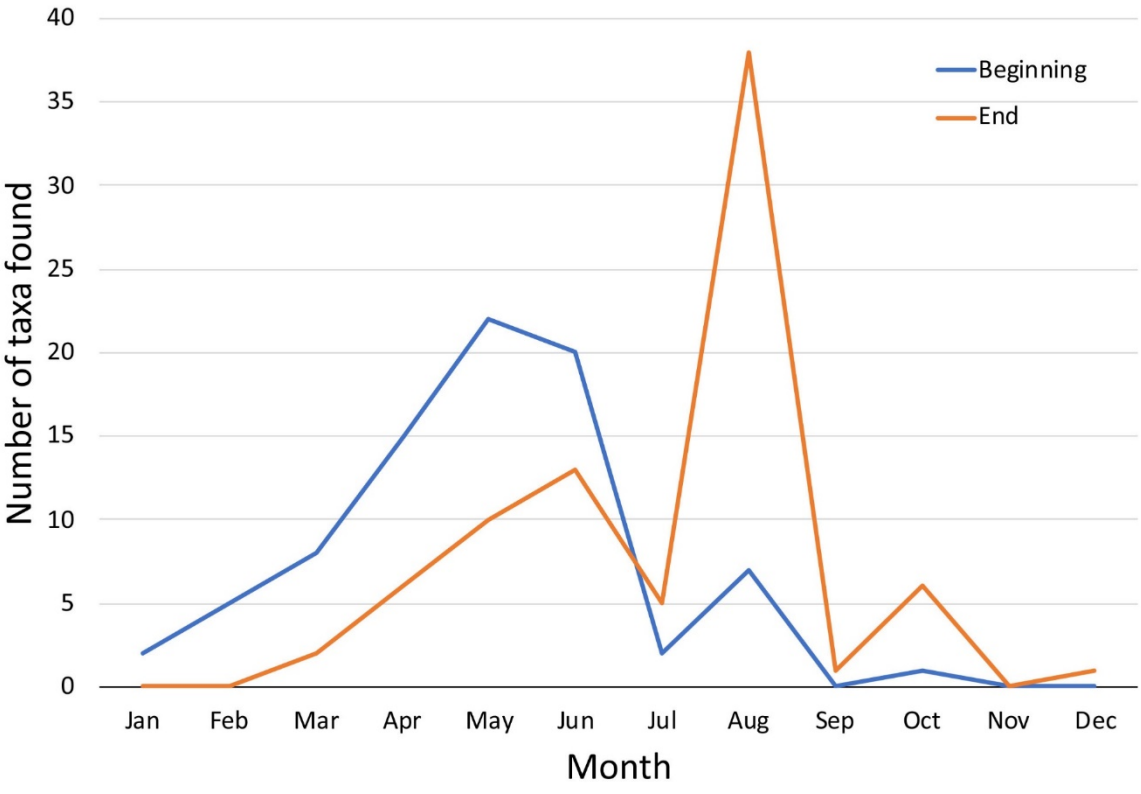

Fig. 5. Data on seasonal occurrence of taxa with planktonic larvae in the Arctic Ocean extracted from published papers (see Table A1). The two curves indicate the beginning (blue) and end (orange) of occurrence.

The differences in mean time between the beginning and the end of occurrence is 63 days, which is a coarse estimate of the mean PLD. Vestfals et al. (2019) reported a PLD for polar cod and saffron cods of 60-90 days but that can be preceded by an egg stage of 35-80 days. For the bivalves *Hiatella arctica* and *Mya truncate,* PLDs of 60-100 and 90 days are reported, respectively (Brandner et al. 2017).

Information about the sample depth was mainly reported rather than vertical profiles of larval abundance. For the few studies that sampled a depth profile, larvae were concentrated in the upper 50 m (e.g. Kuklinski et al. 2013). No study sampled deeper than 200 m.

Based on the very limited input from the literature, it is only possible to use reported data on larval traits as a rough guideline to parameterize the biophysical model. It is also likely that PLD shows interannual variation because of water temperature. The strategy in this work was to include a broad range of parameter values to account for season, drift depth and PLD. This allows the construction of an extensive database of modelled connectivity for many possible parameter combinations, providing flexibility as more empirical data on larval traits become available.

VALIDATION OF THE OCEANOGRAPHIC CIRCULATION MODELS

We do not provide any validation of the ocean models used within this study. The TOPAZ system is an operational model run at the Norwegian Meteorological Institute, and it is an official part of the European Union (marine) Copernicus web portal. Notably, it also contains a data assimilation scheme taking advantage of available observations. The model is used in both a predictive mode (using real time observations) and in a re-analysis mode (using all available data). The model undergoes a continuous validation, for this report the validation of drift buoys is perhaps the most relevant (https://cmems.met.no/ARC-MFC/V2Validation/buoyDrift/index.html). Temperature and salinity are validated here (https://cmems.met.no/ARC-MFC/V2Validation/TSprofile/index.html). Thus, we consider TOPAZ to be well validated. The Arctic4 model does not undergo a similar validation process. The main validation we consider in this study is comparing the Arctic4 to the TOPAZ model, which is well-validated. The two models provide similar results for mean currents and their variability in surface water. In addition, the results from the connectivity matrix analysis does not show significant deviations in strength and direction of dispersion of particles (Fig. 6).

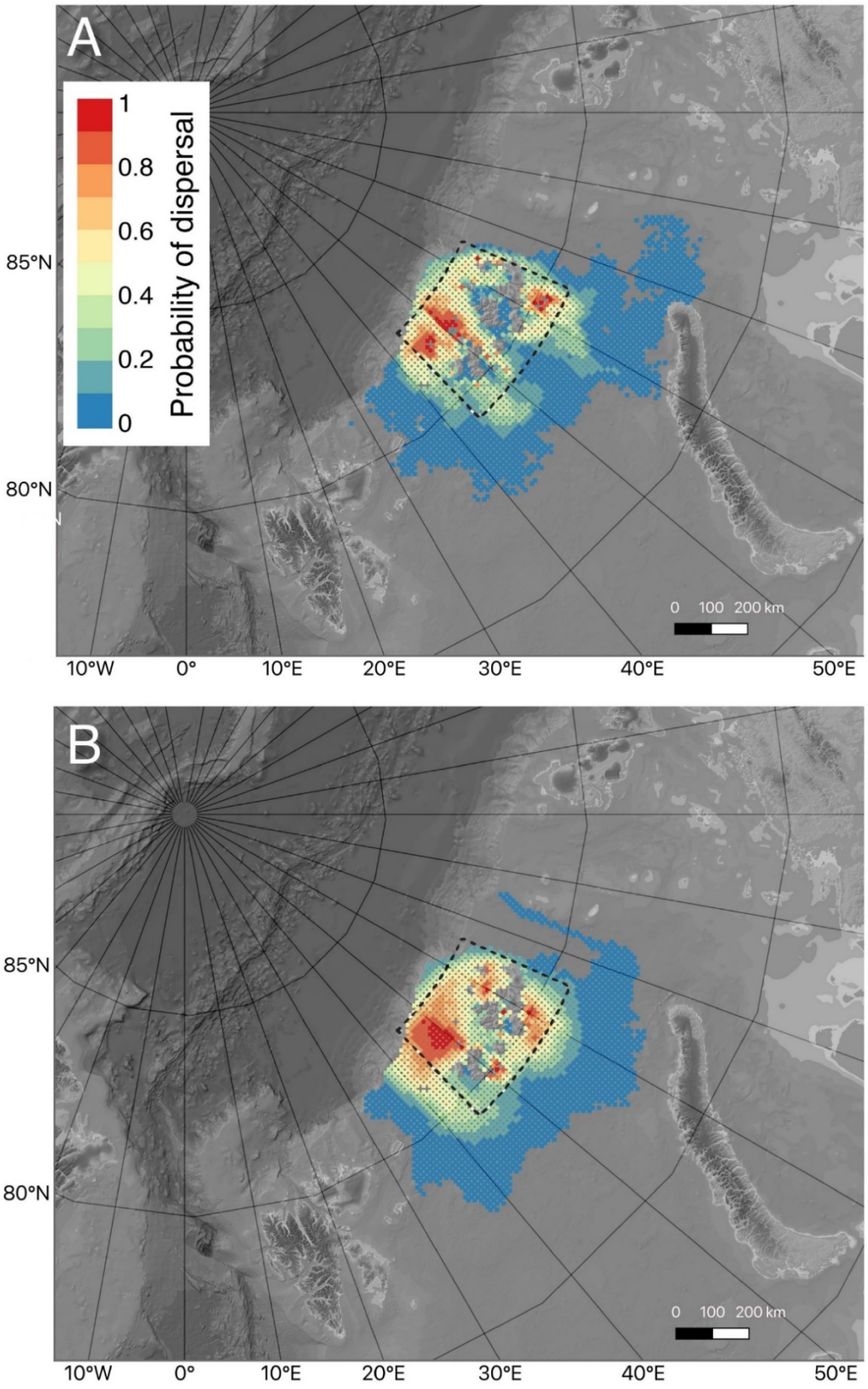

Fig. 6. A comparison of connectivity matrices produced by the two models (A) Arctic4 and (B) TOPAZ. Here particles were seeded within the MPA 238 (Franz Josef Land) shown by the dotted polygon. Probability of dispersal in the surface water with a PLD of 45 days is shown as the colour-coded fields.

LOCAL DISPERSAL DISTANCE AS A FUNCTION OF BIOLOGICAL TRAITS

Modelled dispersal and effects of biological traits are best visualised as a dispersal distance from each release point in the seascape. Figure 7 shows dispersal distance for each of the 40893 grid cells at a drift depth of 10 m and for increasing days of PLD. As expected, dispersal distance increases with PLD, but the distance is also highly dependent on the location in the seascape. In many areas, dispersal distance is less than 100 km but extends to several 100 km along the east Greenland slopes, north of Novaya Zemlya and north of Alaska.

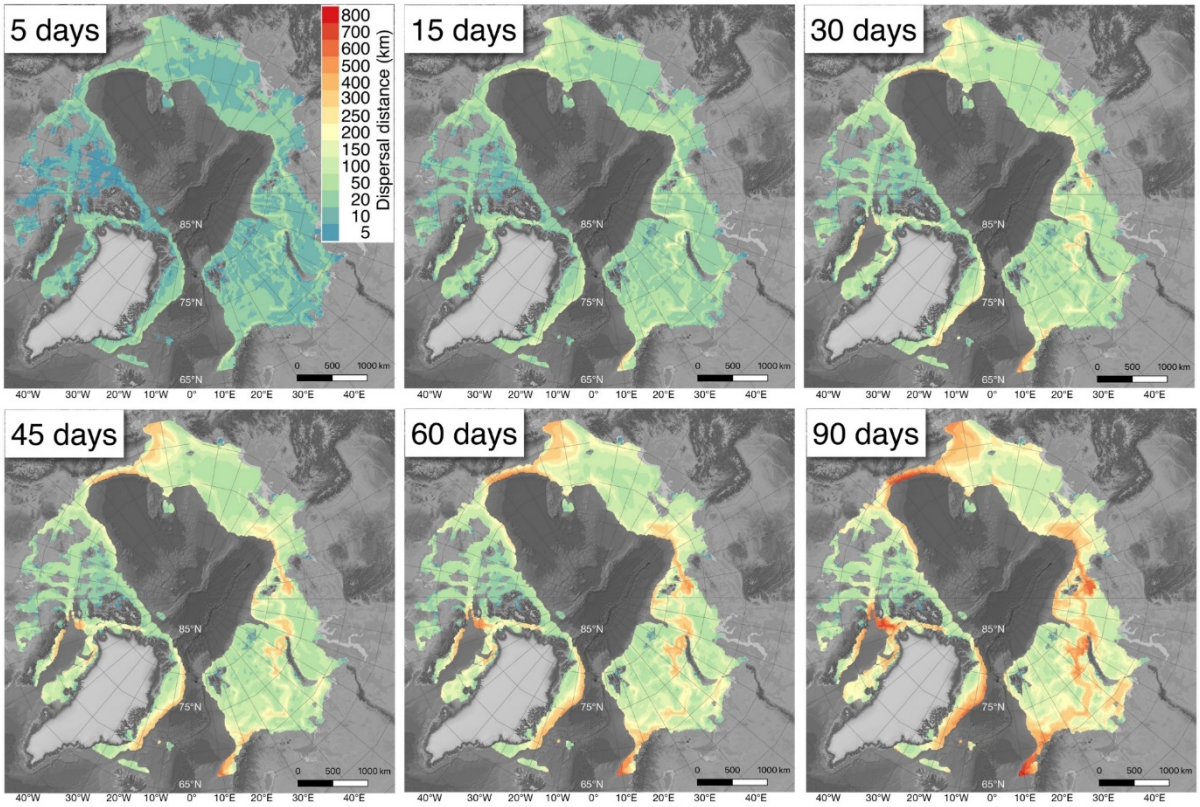

Fig. 7. Maps showing the mean dispersal distance for each of the 40893 grid cells during the warm season (March-October) for Arctic4 modelled larvae drifting at 10 m depth for PLDs of 5, 15, 30, 45, 60 and 90 days. Displayed results are averaged over 10 years (2007 – 2016).

Dispersal distance tends to decrease with increasing depth (Fig. 8), e.g. in the Kara Sea. In most areas, the depth interval explored in the present study (0-150 m) had a modest effect on modelled dispersal distance. This report only presents maps of dispersal distance for a subset of the available connectivity matrices, but these calculations can easily be extended.

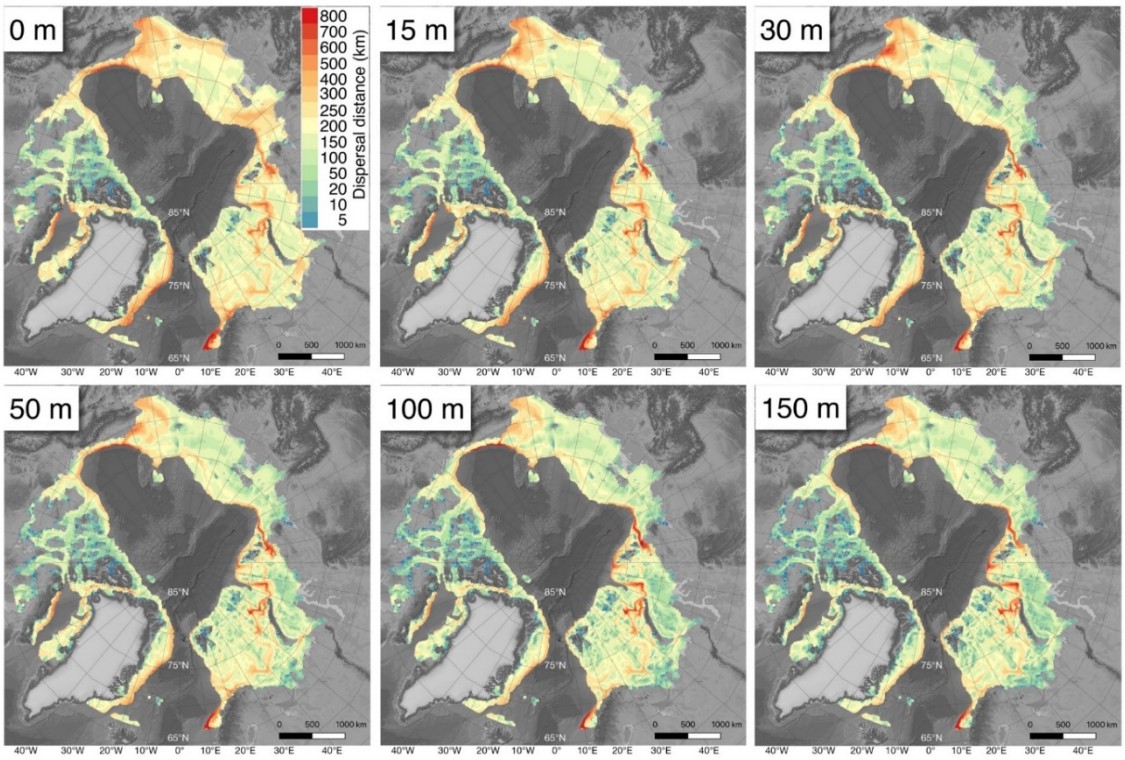

Fig. 8 Maps showing the mean dispersal distance for each of the 40893 grid cells during the warm season (March-October) for Arctic4 modelled larvae drifting at 6 different depths (0, 15, 30, 50, 100 and 150 m) for a PLD of 30 days. Displayed results are averaged over 10 years (2007 – 2016).

IDENTIFICATION OF SOURCES AND SINKS – A BRIEF DEMONSTRATION

In many cases, mores specific information about seascape connectivity compared to dispersal distance is needed. One strategy is to estimate source-sink relationships between areas. For example, this can ascertain how MPAs may function as sources of recruits to ambient areas, to determine the risk of MPAs acting as sinks for contaminants from external sources, or to understand how fish spawning grounds connect via larval dispersal to possible nursery areas. Figures 9 and 10 show a few applications of source-sink analyses for a protected area around Franz Josef Land (CAFF 2013) as an example of how connectivity matrices can be used to identify areas that either deliver larvae to or receive larvae from an MPA. Different MPAs may show very different source patterns as illustrated in Fig. 11 for four selected areas.

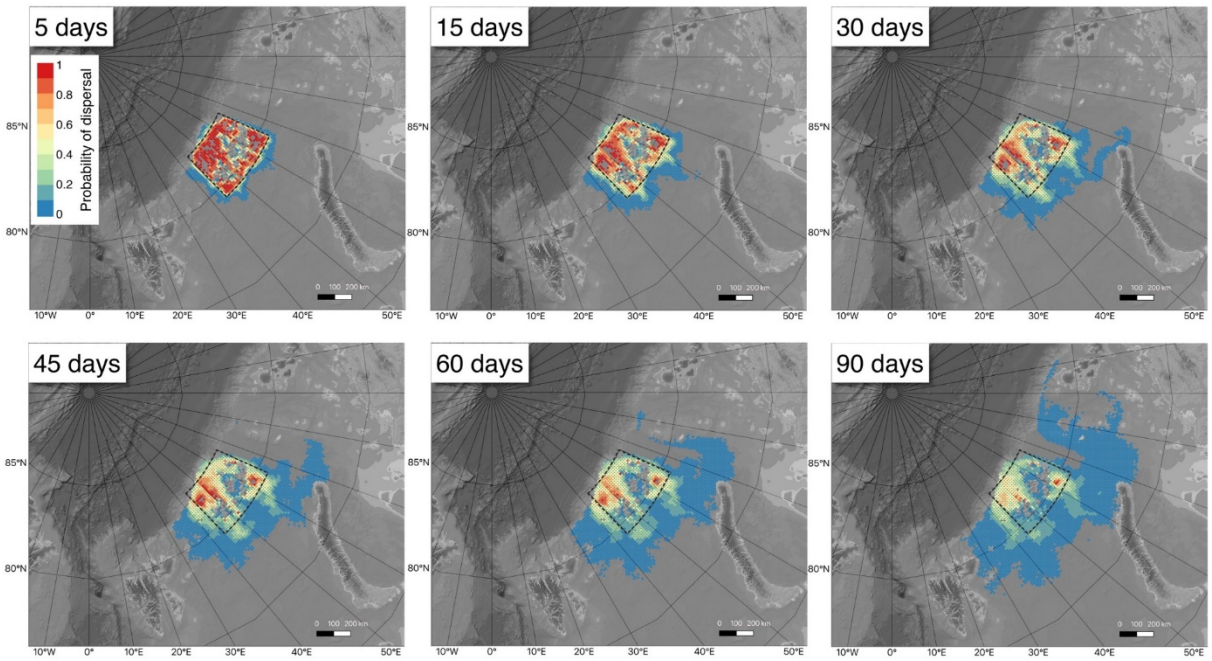

Fig. 9. Areas receiving propagules from the MPA 238 – Frans Josef Land (dotted area), i.e. the MPA acting as a source. The six panels show the effect of increasing PLD. The colour scale (from blue to red) indicates probability (0-1) that a particular model grid receives a propagule originating from the MPA.

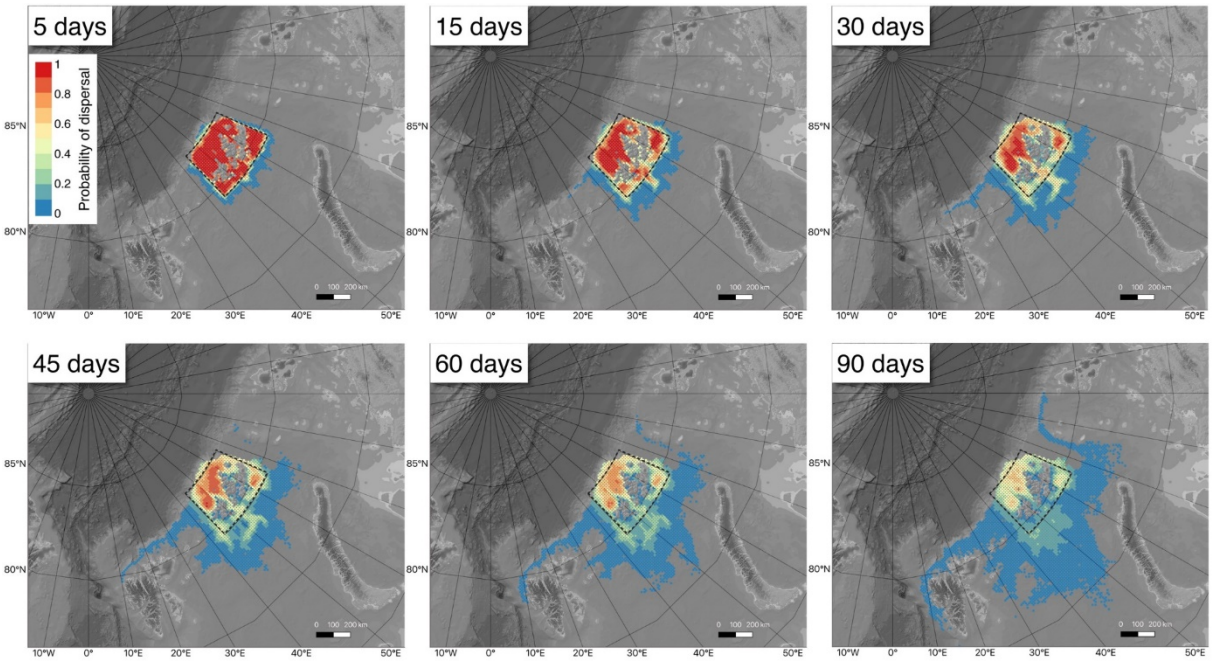

Fig. 10. Areas providing propagules to the MPA 238 – Frans Josef Land (dotted area), i.e. the MPA acting as a sink. The six panels show the effect of increasing PLD. The colour scale (from blue to red) indicates probability (0-1) that a particular model grid receives a propagule originating from the MPA.

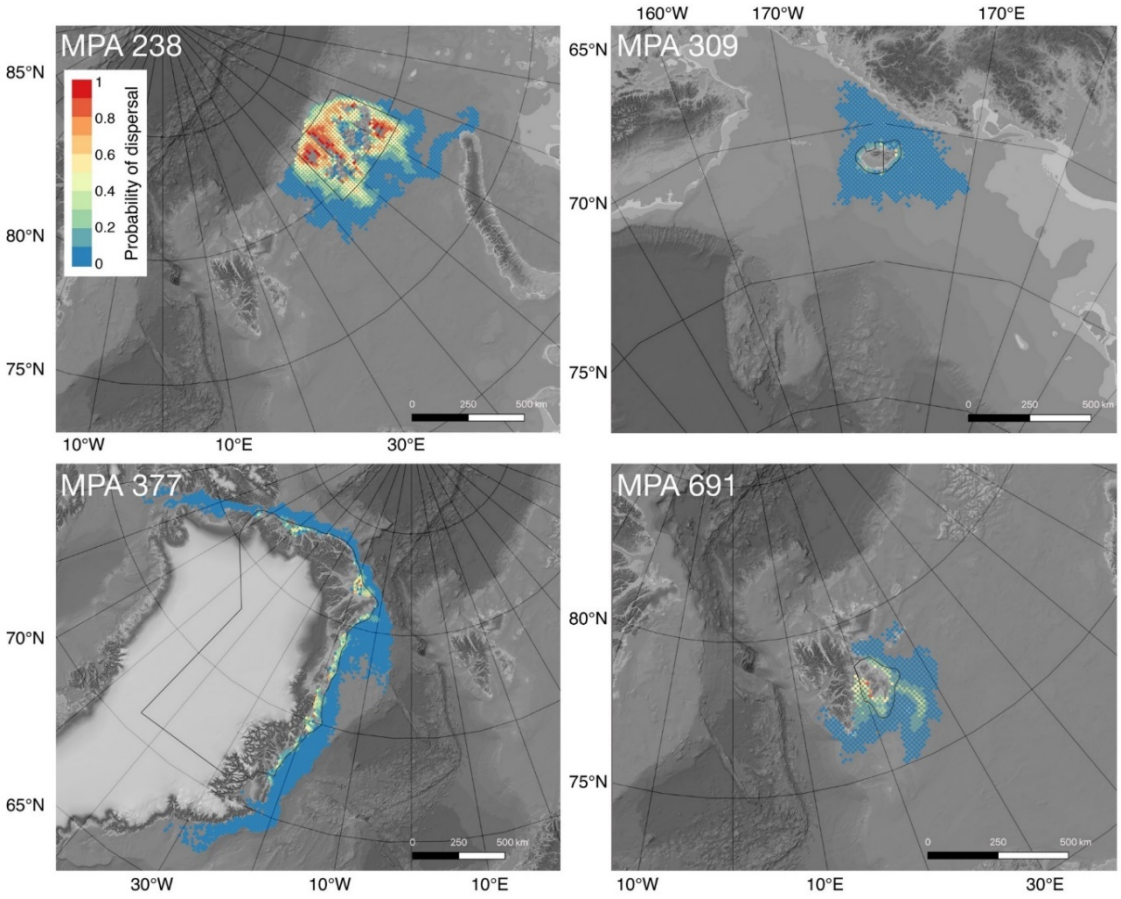

Fig. 11. Areas receiving propagules from 4 selected MPAs (solid polygons, see Fig. 1 for overview). The drift depth was 10 m and the PLD 30 days. The colour scale (from blue to red) indicates relative probability (0 to 1) of propagules originating from the MPA.

EXAMPLES OF LOCAL RETENTION WITH IMPLICATIONS FOR SELF-RECRUITMENT AND PERSISTENCE

A critical aspect in the design of MPAs is the potential for self-recruitment within the designated MPA. For sufficient self-recruitment, a significant portion of released larvae need to be locally retained within the MPA or return to the MPA at the time of settlement. The local retention of released larvae may easily be calculated from the connectivity matrix as the diagonal elements for those grid cells overlapping with the MPA (Eq. 2). It is not well understood what level of self-recruitment that is necessary to maintain persistent populations within an MPA but for many fishes, a level of 40% has been suggested (e.g., Salles et al. 2015) although this could differ between species and areas. Figure 12 shows local retention for the four selected MPAs and for 35 combinations of drift depth and PLD. The variation in dispersal distance (Figs. 7-8) and local retention within MPAs decreases with PLD but is marginally affected by drift depth. There is also an effect of MPA size and shape; the relatively small MPA309 shows low levels of local retention (Fig. 12).

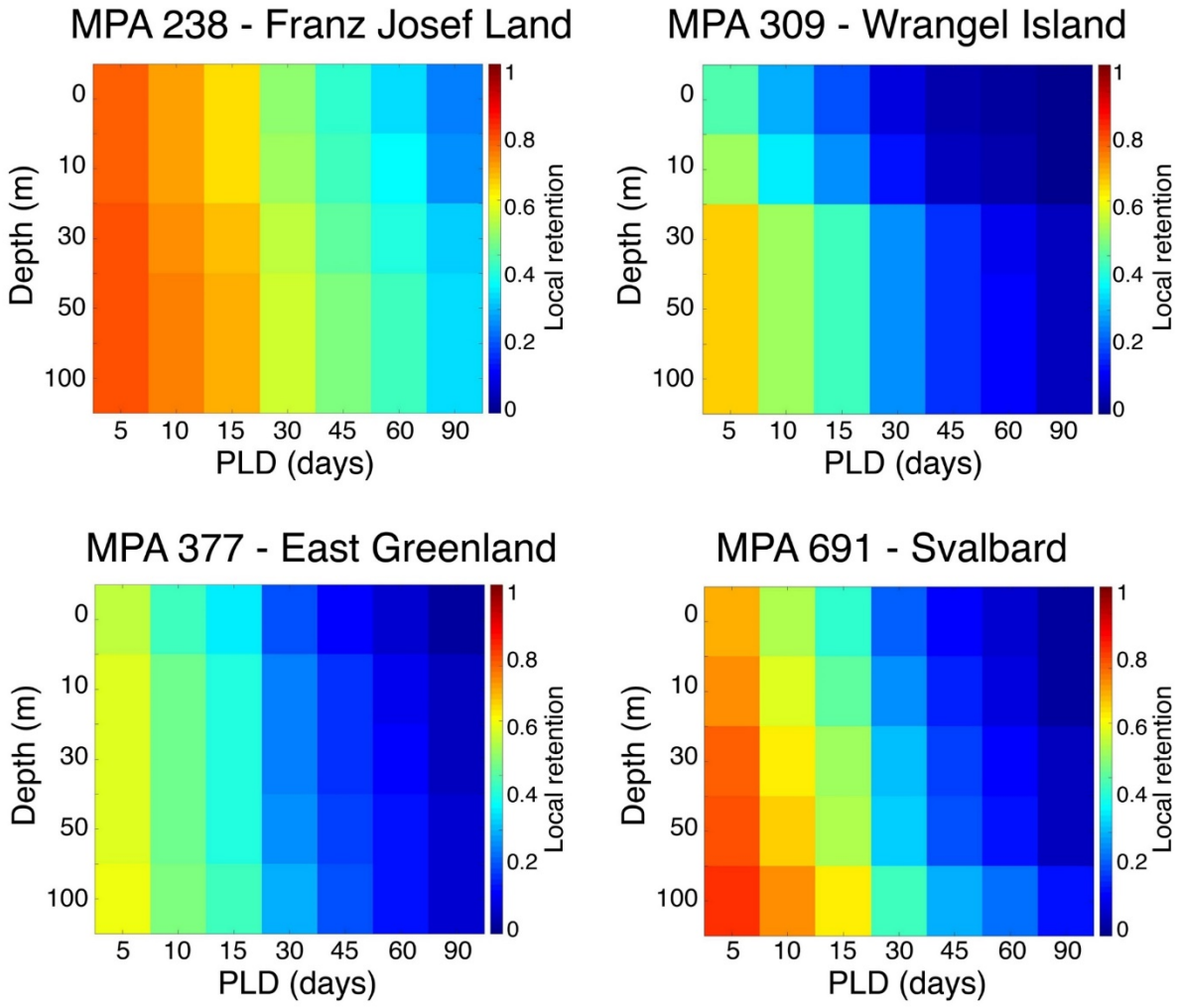

Fig. 12. Graphs showing the local retention (1 is complete retention) in four selected MPAs for larval dispersal at five depths and for seven PLDs.

IDENTIFICATION OF DISPERSAL BARRIERS

We used a cluster method (Nilsson Jacobi et al. 2012) to identify potential dispersal barriers using the connectivity matrices in the domain modelled in the Arctic Ocean. This method requires that the user specifies a threshold for the minimum "leakage" of propagules between partially isolated areas that defines a dispersal barrier. Typically, the connectivity within areas is set to more than 100 times greater than connectivity across barriers. However, this level can be altered depending on the biological process of interest. The potential of genetic differentiation may require strong barriers to gene flow, while demographic independence, e.g. of fish stocks, may develop even when substantial dispersal occurs across barriers. In Fig. 13, four examples are shown of the mapping of connectivity clusters separated by partial dispersal barriers. By increasing the threshold of allowed dispersal across barriers, the domain is partitioned in to more sub-populations. Not surprisingly, by increasing the PLD from 30 to 90 days, the areas of high internal connectivity increase in size. The open shelf areas show few barriers with large areas that have high internal connectivity, e.g. the Kara Sea. In contrast, the more complex geomorphology of the Canadian Arctic Archipelago, however, leads to more dispersal barriers.

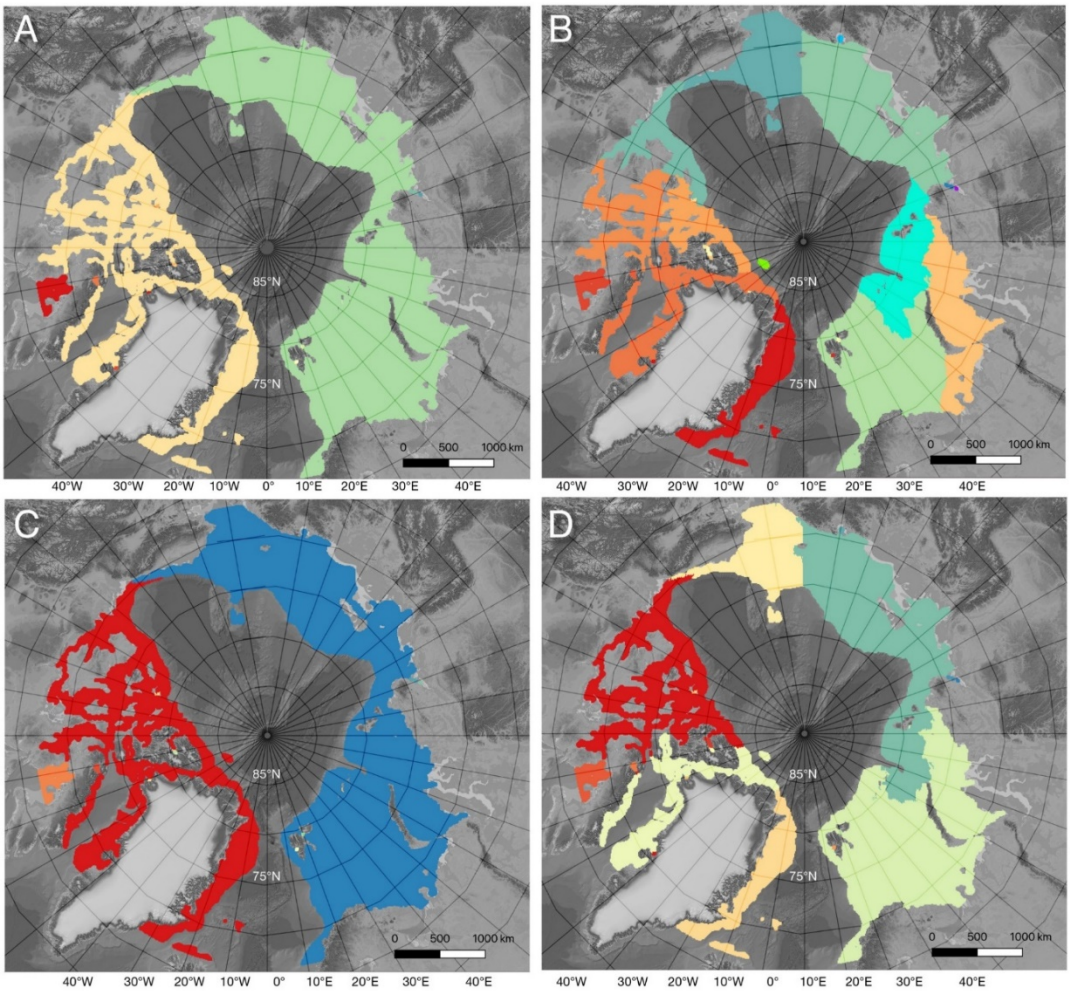

Fig. 13. Identification of dispersal barriers on the Arctic Ocean shelf based on the biophysical model of larval dispersal for some dispersal trait combinations. The top panels show barriers for dispersal at 10 m depth with a PLD of 30 days and with a threshold of dispersal across barriers of (A) 0.0007 and (B) 0.01. The bottom panels show barriers for dispersal at 10 m depth with a PLD of 90 days and with a threshold of dispersal across barriers of (C) 0.0009 and (D) 0.01 Colour transitions between areas indicate partial dispersal barriers. Colours are arbitrarily chosen.

TEMPORAL VARIABILITY AND TRENDS OF CONNECTIVITY METRICS

The modelled connectivity metrics, dispersal distance and local retention, generally show a seasonal variation with longer average dispersal distance and lower local retention within MPAs during the warmer season (Fig. 14). However, the annual variation in surface water from 1991 to 2015 is considerable as shown by large standard deviations for each month (Fig. 14).

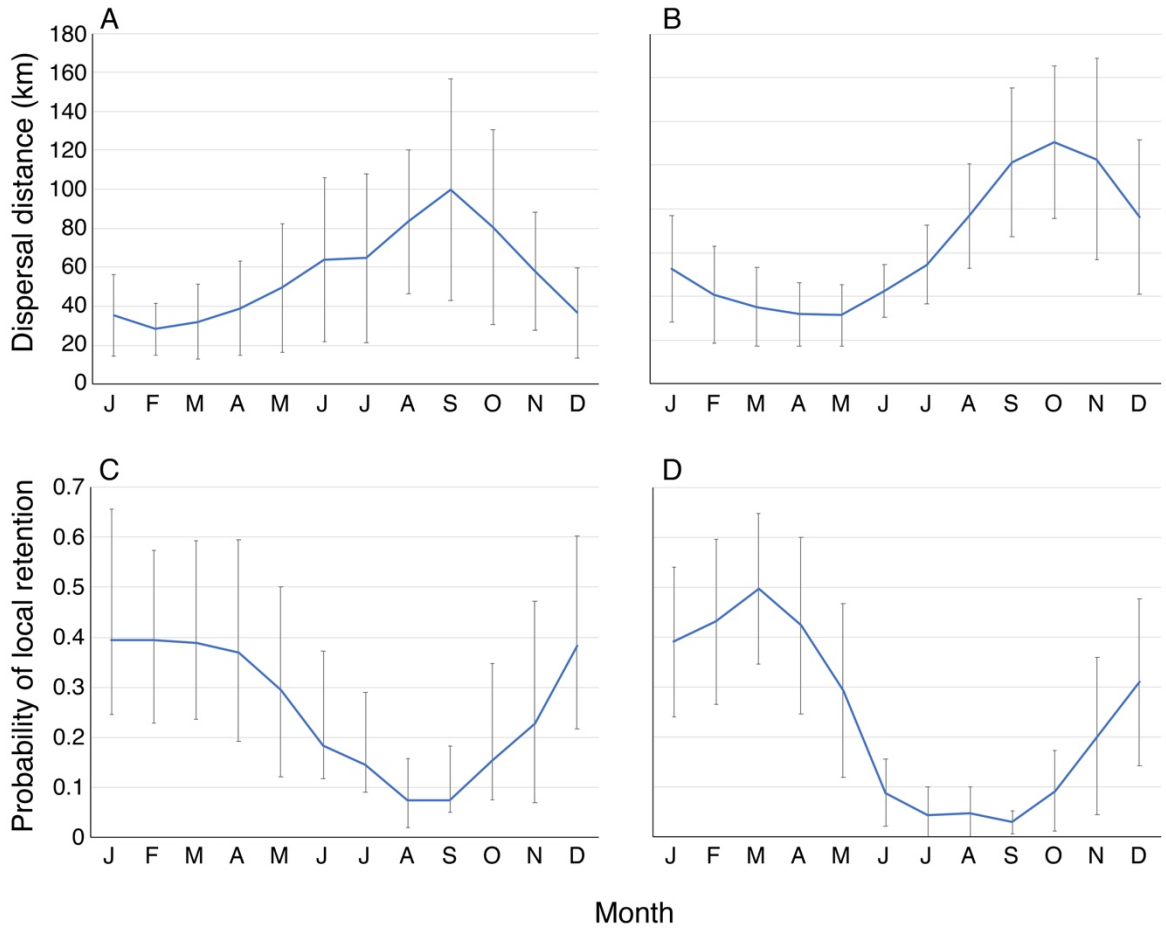

Fig. 14. Seasonal variation (mean ± SD, n=25) in modelled connectivity metrics in surface water (PLD: 30 days) between 1991 and 2015 for two selected MPAs (A) dispersal distance for MPA 196, (B) dispersal distance for MPA 376, (C) local retention for MPA 196, (D) local retention for MPA 376.

The climate of the Arctic Ocean has changed significantly during the past two decades (Meredith et al. 2019). In the ocean this is most obvious as a trend of receding sea ice cover during the warm season with unprecedently low cover in 2012 and 2020 in a time series beginning in 1978 (National Snow and Ice Data Center 2019). The trend of reduced sea ice cover is also evident in the TOPAZ model although annual variability is high (Fig. 15).

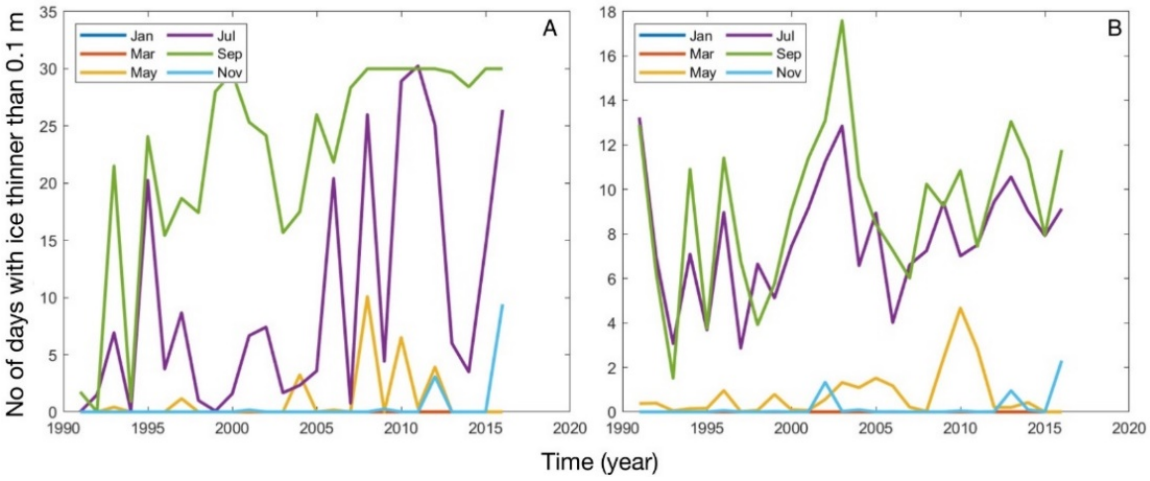

Fig. 15. Temporal variability of ice cover from the TOPAZ model showing the number of days per month with ice thinner than 0.1 m for model grid cells within (A) MPA 196, and (B) MPA 377.

In Fig. 16 the temporal variation from 1991 to 2015 of modelled dispersal distance and local retention in surface water is shown for two MPAs and for each month separately. There is again considerable annual variation and clear trends across the time period are generally not obvious although there are statistically significant trends for some months and MPAs (Figs. 16 and 17). Table 1 shows a summary of the trend analyses with linear regression for seven selected MPAs. A potential pattern is that most of the significant trends occur during the warm season, which correlates to the receding sea ice cover. For five of the MPAs the local retention shows a negative trend, while for two MPAs the trend is positive, tentatively suggesting that the change in sea ice cover may have different effects on connectivity in different areas. The general negative trend in local retention in MPAs is consistent with the lower retention during the warm season as seen in Fig. 14.

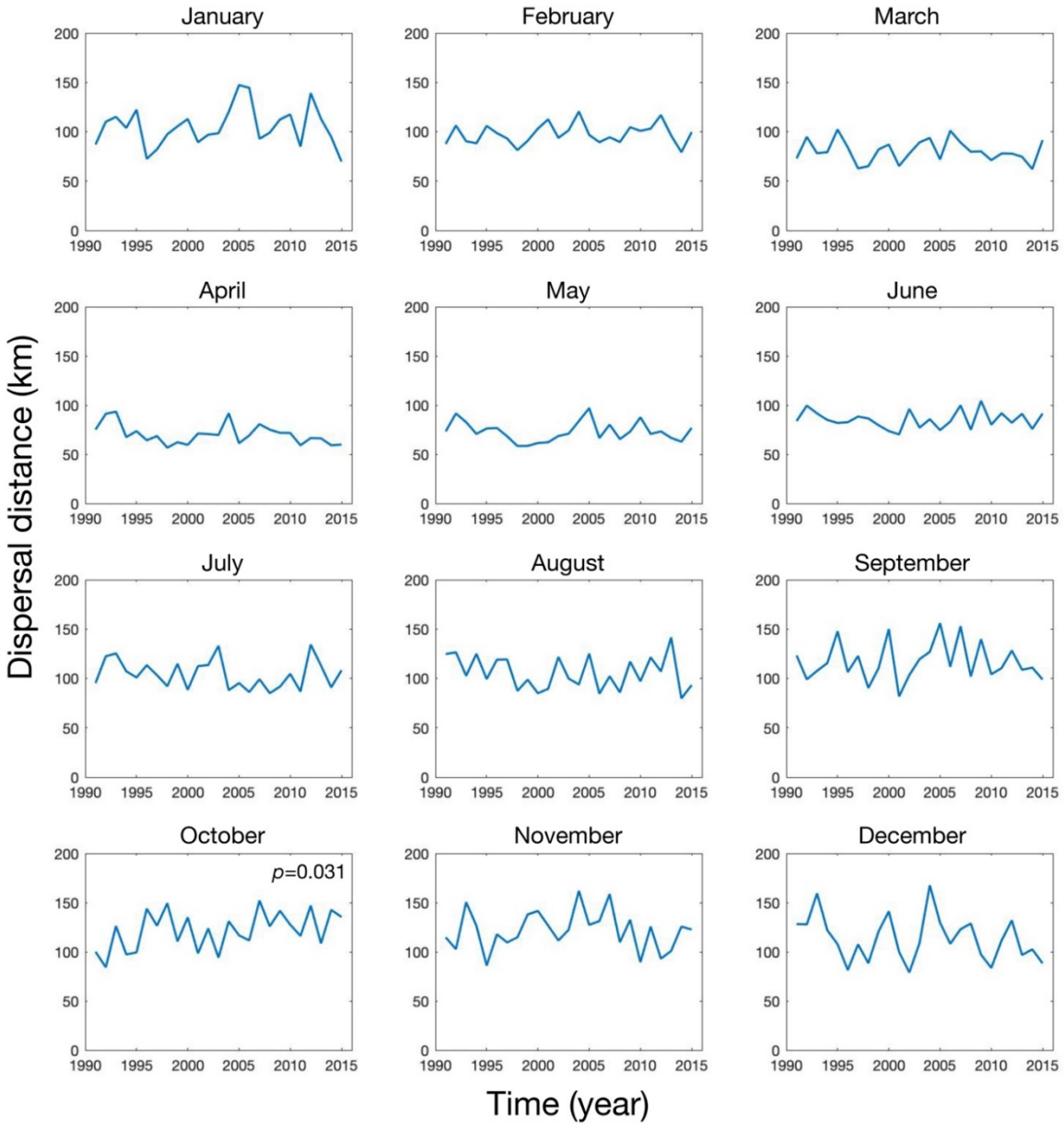

Fig. 16. Temporal variability for each month in mean dispersal distance in surface water (PLD: 30 days) between 1991 and 2015 for MPA 309. Also shown is any significant trend (p<0.05) based on a linear regression analysis.

Table 1. Linear regression analysis of temporal trends from 1991 to 2015 in modelled connectivity metrics, dispersal distance and local retention, for seven selected CAFF MPAs. For each MPA it is shown which month showed a significant trend (p<0.05), and if the slope is positive or negative.

Dispersal distance						
MPA 196	**MPA 238**	**MPA 309**	**MPA 376**	**MPA 377**	**MPA 691**	**MPA 1433**
None	Sep, negative, *p*=0.04	Oct, positive, *p*=0.031	None	Jun, negative, *p*=0.0007 Jul, negative, *p*=0.0009 Aug, negative, *p*=0.0005	Oct, negative, *p*=0.001 Dec, negative, *p*=0.028	Oct, positive, *p*=0.029
Local retention						
MPA 196	**MPA 238**	**MPA 309**	**MPA 376**	**MPA 377**	**MPA 691**	**MPA 1433**
Sep, negative, *p*=0.028	May, negative, *p*=0.042	Oct, negative, *p*=0.036	May, negative, *p*=0.006 Jun, negative, *p*=0.0001 Jul, negative, *p*=0.01	Jul, positive, *p*=0.001 Aug, positive, *p*=0.036	Mar, negative, *p*=0.045 Oct, positive, *p*=0.008 Dec, positive, *p*=0.00¢1	Oct, negative, *p*=0.03

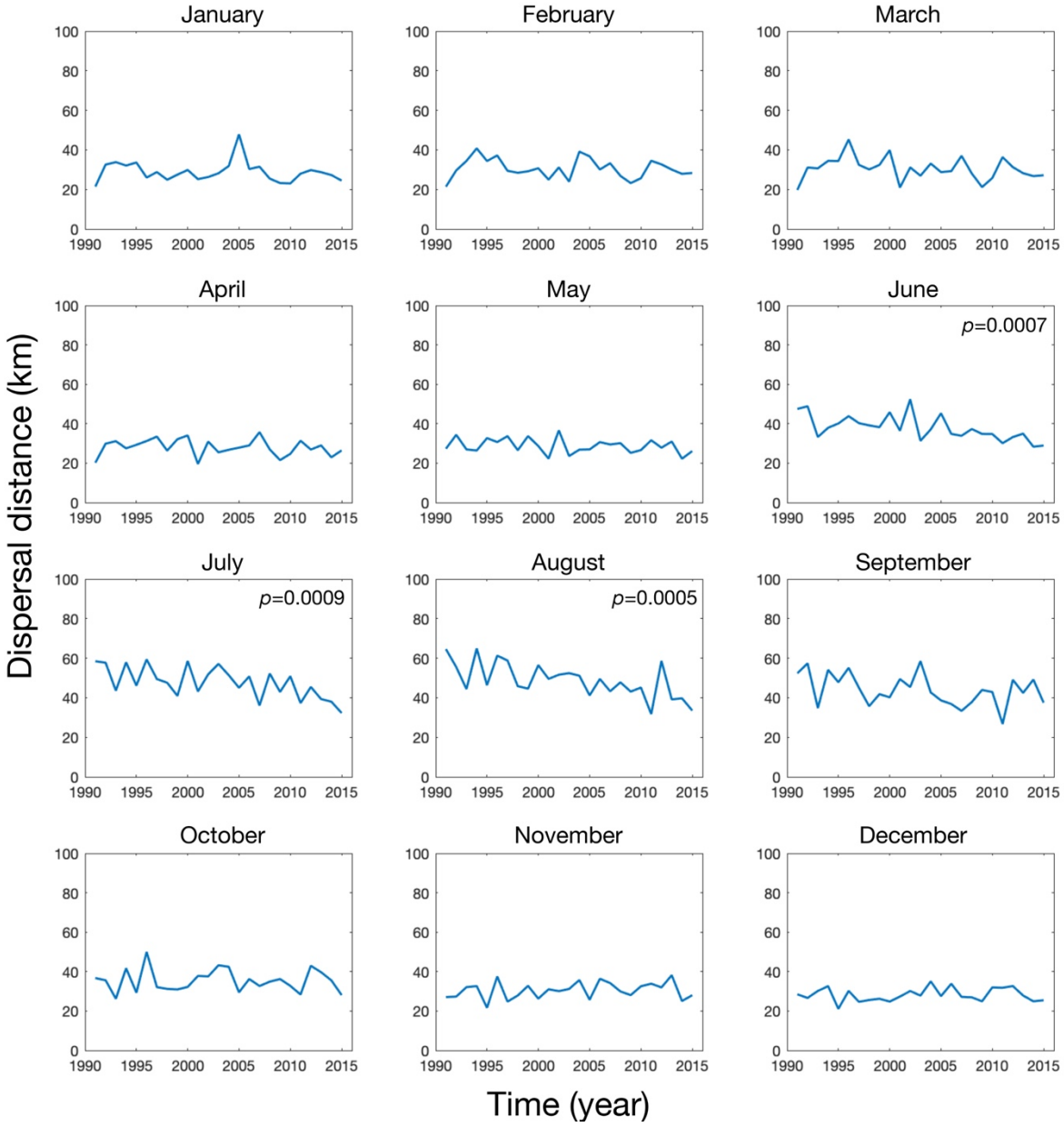

Fig. 17. Temporal variability for each month in mean dispersal distance in surface water (PLD: 30 days) between 1991 and 2015 for MPA 377. Also shown is any significant trend (p<0.05) based on a linear regression analysis.

VI. CONCLUSIONS AND FUTURE PERSPECTIVES

In this project we used a biophysical model to estimate seascape connectivity within the continental shelf of the Arctic Ocean with a focus on organisms dispersing with free-drifting larvae. The set of tools described here to assess seascape connectivity are based on biophysical modelling of larval dispersal and is mainly relevant for organisms with sedentary adults where connectivity largely depends on physical water transport of eggs, larvae or other propagules. A large number of dispersal trajectories were simulated using including many combinations of spawning season, drift depth and pelagic larval duration (PLD). We used two ocean circulation models (Arctic4 and TOPAZ) for our dispersal simulations, which provided similar results for the connectivity between grid cells in the model domain. Simulation results are primarily stored as connectivity matrices, which comprise a database of dispersal probability between 40893 selected grid cells in the model. In this report we have demonstrated how these connectivity matrices can be incorporated as tools for analyses and design of proposed or existing MPAs. Increasingly, MPAs are designed as ecologically coherent networks (HELCOM 2016) and the toolbox demonstrated here can be used to assess the relevant size and shape of individual MPAs (i.e. their adequacy) and how they act as a network based on connectivity, both within the network and within non-protected habitat (Jonsson et al. 2020).

Dispersal distance is more sensitive to increasing PLD and less influenced of the drift depth. The preliminary analysis indicates that expected dispersal distance in the Arctic Ocean may be greater for a given PLD than in some previously modelled coastal areas in the North Sea (Jonsson et al. 2016) and in the Baltic Sea (Jonsson et al. 2020). Generally, the many open coastal areas may explain this more extensive dispersal. In some areas where the coast is complex (e.g. the Canadian Arctic Archipelago), dispersal distance is more modest. The generally large dispersal distance per day and also the expected long PLDs in cold waters (e.g. Vestfals et al. 2019) imply that MPAs need to be relatively large to ensure a high level of local retention and self-recruitment.

The connectivity matrix further provides a flexible method to identify sources and sinks to a specified area, e.g. MPAs. Sources here may be areas that supply an MPA with recruits, but may also include areas that cause environmental impact on protected areas, e.g. sources of non-indigenous species that compete with native species, discharge of contaminants or oil spills. The latter may become increasingly important as the Arctic warms, as reductions in sea ice will open the Northwest Passage to shipping, and where new gas and oil reserves can be found and exploited. Thus, it is clear that activities in a considerable area outside an MPA may affect the conditions within the boundaries of MPAs due to source-sink dynamics. However, the shape of this external area will depend on the local circulation pattern. The source area will be a function of PLD, the depth of dispersal and seasonal variation in circulation. Similarly, it is easy to extract from the connectivity matrix the probability that fertilized eggs, larvae or other propagules released within an MPA will also settle within that MPA. High local retention may lead to a largely self-recruited, closed local population, which may persist without immigration from other protected or unprotected local populations.

Connectivity patterns in the seascape (e.g. specified by a connectivity matrix), may reveal areas with high internal connectivity with partial dispersal barriers to other such areas. Barriers may indicate demographically independent local populations (stocks) or genetically differentiated populations with local adaptations if barriers are sufficiently strong (Allendorf et al. 2013). Based on the connectivity matrix,

well-connected clusters can be identified to minimize the total dispersal (leakage) among such groups and subjected to some penalty of aggregating groups (Nilsson Jacobi et al. 2012). This tool visualizes the structure of the connectivity matrix by projecting it onto a geographic map. Colour-coded areas may indicate biologically relevant management units (Palsbøll et al. 2007) separated by dispersal barriers. Dispersal barriers are generally partial and the number of dispersal barriers decrease as less dispersal is allowed across barriers, which is specified by the user. Genetically differentiated local populations are expected to be associated with fewer but stronger barriers (Jahnke et al. 2018), while a larger number of more "leaky" barriers may represent the distribution of demographically independent stocks. Such local populations or stocks may require separate conservation and management actions, and the establishment of MPAs may be stratified across such management units.

The analyses of temporal variability and tests for temporal trends of modelled dispersal distance and local retention, not surprisingly, showed large annual variability but with a clear seasonal pattern. Interestingly, there are some significant trends (1991-2015) of connectivity metrics during the warm season, which correlate with the receding sea ice cover. The ongoing warming of the sea may also affect connectivity through a decrease in PLD caused by higher metabolism and faster maturation to settling competency (O'Connor et al. 2007).

As a future perspective, it will now be possible to apply the modelled connectivity matrices in network analyses of complete MPA networks using a metapopulation perspective (Jonsson et al. 2020). We have previously developed a framework based on Eigenvalue Perturbation Theory (EPT, Ovaskainen & Hanski 2003, Nilsson Jacobi & Jonsson 2011). Connectivity is here directly linked to metapopulation dynamics to identify optimal MPA networks with respect to connectivity. By applying EPT to the connectivity matrix, it is possible to identify the best network of MPAs that maximizes the growth rate of the global metapopulation (protected and unprotected areas) when the metapopulation is small, which is typical of threatened species. One advantage of this approach is that there is a unique network of MPAs for each connectivity matrix and the total protected area, so that this network is directly linked to persistence of the whole metapopulation. Connectivity is one among several aspects that need to be considered in MPA design, e.g. habitat distribution and quality (Virtanen et al. 2018). If habitat information is available (e.g. presence-absence or habitat quality) it is possible combine this with the connectivity matrix (Berglund et al. 2012,). It is also possible to identify consensus MPA networks targeting multiple species with different dispersal strategies (Jonsson et al. 2016).

There are several limitations in the present study and future research may improve our view of Arctic connectivity. The oceanographic models used here are still rather coarse and does not resolve shallow areas and complex coastlines. More highly resolved oceanographic models can be used in regional analyses of connectivity. A future prospect is also to use projections of ocean currents to estimate future connectivity assuming different climate change scenarios. The modelled dispersal in this report may be viewed as a hypothesis of Arctic connectivity. Future empirical studies will be highly valuable to test model predictions, e.g. of dispersal barriers. The increasing use of genomic methods are here be especially promising. Finally, we again emphasize that this study offers modelled connectivity relevant for those marine species that mainly disperse with ocean currents. Other species, mainly marine mammals and birds, show different modes of dispersal and connectivity based on active migration and require other methods, e.g. tagging and genetic markers.

The database of connectivity matrices produced in this project together with the demonstration of suitable analytical methods will hopefully add to the PAME's MPA toolbox.

VII. DATA AVAILABILITY

The primary data produced within this project consist of a set of connectivity matrices specifying the probability of dispersal within the studied seascape for combinations of year, month, drift depth and pelagic larval duration (drift duration in days). Each connectivity matrix has a data structure of 40893 rows and columns and is saved as sparse matrices in Matlab .mat binary format. In total there are 9960 connectivity matrices based on the Arctic4 model and 2016 matrices based on the TOPAZ model. Each connectivity matrix requires around 1 MB of digital memory. There is also a set of 126 aggregated connectivity matrices which are averaged over all years and divided into two seasons (March-October and November-February). Aggregated connectivity matrices based on Arctic4 are available for the depths 0, 10, 15, 30, 50, 70, 100 and 150 m, and for the PLDs 5, 10, 15, 30, 45, 60 and 90 days. For TOPAZ there are aggregated connectivity matrices for 0 m depth, and for the PLDs 5, 10, 15, 30, 45, 60 and 90 days. The aggregated connectivity matrices each requires between 10-50 MB of digital memory.

In addition to the primary data in the form of connectivity matrices there are derived datasets based on the connectivity matrices. First there are results from the barrier analysis assigning each of the 40893 locations included in the model domain to a cluster of high within-cluster connectivity. This analysis was performed for a large set of aggregated connectivity matrices and for a range of parameters representing the level of allowed dispersal between clusters. In total there are 2149 files (.txt) representing combinations of drift depth, PLD and allowed dispersal between clusters. Second, there are visualisations of data in the form of maps, many of them included in this report. The maps are available as shape files.

The intention is that all or selected data could be open access, if an infrastructure for storage and downloading can be arranged.

IX. REFERENCES

Allendorf, F. W., G. H. Luikart, and S. N. Aitken. 2013. Conservation and the genetics of populations. John Wiley & Sons.

Berglund, M., M. Nilsson Jacobi, and P. R. Jonsson. 2012. Optimal selection of marine protected areas based on connectivity and habitat quality. Ecological Modelling **240**:105-112.

Brandner, M. M., E. Stübner, A. J. Reed, T. M. Gabrielsen, and S. Thatje. 2017. Seasonality of bivalve larvae within a high Arctic fjord. Polar Biology **40**:263-276.

CAFF. 2013. Arctic Biodiversity Assessment. Status and trends in Arctic biodiversity. Akureyri.

Corell, H., P. O. Moksnes, A. Engqvist, K. Döös, and P. R. Jonsson. 2012. Depth distribution of larvae critically affects their dispersal and the efficiency of marine protected areas. Marine Ecology Progress Series **467**:29-46.

Cowen, R. K., and S. Sponaugle. 2009. Larval dispersal and marine connectivity. Annual Review of Marine Science **1**:443-466.

HELCOM. 2016. Ecological coherence assessment of the Marine Protected Area network in the Bal c Sea. Baltic Sea Environment Proceedings **148**:74 pp.

Jahnke, M., P. R. Jonsson, P. O. Moksnes, L. O. Loo, M. Nilsson Jacobi, and J. L. Olsen. 2018. Seascape genetics and biophysical connectivity modelling support conservation of the seagrass *Zostera marina* in the eastern North Sea. Evolutionary Applications **11**:645-661.

Jonsson, P. R., P. O. Moksnes, H. Corell, E. Bonsdorff, and M. Nilsson Jacobi. 2020. Ecological coherence of Marine Protected Areas: New tools applied to the Baltic Sea network. Aquatic Conservation: Marine and Freshwater Ecosystems **30**:743-760.

Jonsson, P. R., M. Nilsson Jacobi, and P. O. Moksnes. 2016. How to select networks of marine protected areas for multiple species with different dispersal strategies. Diversity and Distributions **22**:161-173.

Jorde, P. E., G. Sovik, J. I. Westgaard, J. Albretsen, C. Andre, C. Hvingel, T. Johansen, A. D. Sandvik, M. Kingsley, and K. E. Jorstad. 2015. Genetically distinct populations of northern shrimp, Pandalus borealis, in the North Atlantic: adaptation to different temperatures as an isolation factor. Molecular Ecology **24**:1742-1757.

Kuklinski , P., J. Berge, L. McFadden, K. Dmoch, M. Zajaczkowski, H. Nygård, K. Piwosz, and A. Tatarek. 2013. Seasonality of occurrence and recruitment of Arctic marine benthic invertebrate larvae in relation to environmental variables. Polar Biology **36**:549-560.

Lester, S. E., and B. S. Halpern. 2008. Biological responses in marine no-take reserves versus partially protected areas. Marine Ecology Progress Series **367**:49-56.

Meredith, M., M. Sommerkorn, S. Cassotta, C. Derksen, A. Ekaykin, A. Hollowed, G. Kofinas, A. Mackintosh, J. Melbourne-Thomas, M. M. C. Muelbert, G. Ottersen, H. Pritchard, and E. A. G. Schuur. 2019. Polar Regions. *in* H.-O. Pörtner, D. C. Roberts, V. Masson-Delmotte, P. Zhai, M. Tignor, E. Poloczanska, K. Mintenbeck, A. Alegría, M. Nicolai, A. Okem, J. Petzold, B. Rama, and N. M. Weyer, editors. IPCC Special Report on the Ocean and Cryosphere in a Changing Climate. The Intergovernmental Panel on Climate Change.

Micheli, F., A. Saenz-Arroyo, A. Greenley, L. Vazquez, J. A. Espinoza Montes, M. Rossetto, and G. A. De Leo. 2012. Evidence that marine reserves enhance resilience to climatic impacts. PLoS ONE **7**:e40832.

Mokses, P. O., H. Corell, K. Tryman, R. Hordoir, and P. R. Jonsson. 2014. Larval behavior and dispersal mechanisms in shore crab larvae (*Carcinus maenas*): Local adaptations to different tidal environments? Limnology and Oceanography **59**:588-602.

National Snow and Ice Data Center. 2019. Arctic sea and ice news & analysis. https://nsidc.org/arcticseaicenews/charctic-interactive-sea-ice-graph/, accessed August 21, 2020.

Nilsson Jacobi, M., C. André, K. Döös, and P. R. Jonsson. 2012. Identification of subpopulations from connectivity matrices. Ecography **35**:1004-1016.

Nilsson Jacobi, M., and P. R. Jonsson. 2011. Optimal networks of nature reserves can be found through eigenvalue perturbation theory of the connectivity matrix. Ecological Applications **21**:1861-1870.

O'Connor, M. I., J. F. Bruno, S. D. Gaines, B. S. Halpern, S. E. Lester, B. P. Kinlan, and J. M. Weiss. 2007. Temperature control of larval dispersal and the implications for marine ecology, evolution, and conservation. Proceedings of the National Academy of Sciences **104**:1266-1271.

OSPAR. 2013. An assessment of the ecological coherence of the OSPAR Network of Marine Protected Areas in 2012. OSPAR Commission, London.

Ovaskainen, O., and I. Hanski. 2003. How much does an individual habitat fragment contribute to metapopulation dynamics and persistence? Theoretical Population Biology **64**:481-495.

Palsbøll, P. J., M. Bérubé, and F. W. Allendorf. 2007. Identification of management units using population genetic data. Trends in Ecology and Evolution **22**:11-16.

PAME. 2015. Framework for a pan-arctic network of marine protected areas. Protection of the Arctic Marine Environment (PAME).

Salles, O. C., J. A. Maynard, M. Joannides, C. M. Barbu, P. Saenz-Agudelo, G. R. Almany, M. L. Berumen, S. R. Thorrold, G. P. Jones, and S. Planes. 2015. Coral reef fish populations can persist without immigration. Proceedings of the Royal Society B **282**:20151311.

van Sebille, E., S. M. Griffies, R. Abernathey, T. P. Adams, P. Berloff, A. Biastoch, B. Blanke, E. P. Chassignet, Y. Cheng, C. J. Cotter, E. Deleersnijder, K. Döös, H. F. Drake, S. Drijfhout, S. F. Gary, A. W. Heemink, J. Kjellsson, I. M. Koszalka, M. Lange, C. Lique, G. A. MacGilchrist, R. Marsh, C. G. M. Adame, R. McAdam, F. Nencioli, C. B. Paris, M.

D. Piggott, J. A. Polton, S. Ruhs, S. H. A. M. Shah, M. D. Thomas, J. B. Wang, P. J. Wolfram, L. Zanna, and J. D. Zika. 2018. Lagrangian ocean analysis: Fundamentals and practices. Ocean Modelling **121**:49-75.

Vestfals, C. D., F. J. Mueter, J. T. Duffy-Anderson, M. S. Busby, and A. De Robertis. 2019. Spatio-temporal distribution of polar cod (*Boreogadus saida*) and saffron cod (Eleginus gracilis) early life stages in the Pacific Arctic. Polar Biology **42**:969-990.

Virtanen, E. A., M. Viitasalo, J. Lappalainen, and A. Moilanen. 2018. Evaluation, gap analysis, and potential expansion of the Finnish marine protected area network. Frontiers in Marine Science **5**:402.

Watson, J. R., S. Mitarai, D. A. Siegel, J. E. Caselle, C. Dong, and J. C. McWilliams. 2010. Realized and potential larval connectivity in the Southern California Bight. Marine Ecology Progress Series **401**:31-48.

APPENDIX (ATTACHED)

- Table A1. Extracted data from a literature review of traits relevant for dispersal of invertebrate and fish larvae.

			Larval type		Depth distribution (m) %					Spawning season from	Spawning season to	Larval season from	Larval season to	Larval peak	Larval interval	Peak hatching	Egg PLD	Larval PLD	Adult habitat	Source area	Reference
Phylum /Class	Order /Family	Species /Stage	Pelagic /Benthic	Depth of occurrence (m)	0-20	20-50	50-100	100-200	>200	(month)		(month)	(month)	(month)	(days)	(month)	(days)	(days)			
Pisces	Gadiformes	*Boreogadus saida*	P	surface	100					1	2	2	4			May-June	35-79	60-90		Chuckchi Sea	Ref in Vestfals et al. (2019)
Pisces	Gadiformes	*Eleginus gracilis*	P	surface	100					1	2	2	4			April-May	33-90	60-90		Chuckchi Sea	Ref in Vestfals et al. (2019)
Bivalvia	Adepodonta	*Hiatella arctica*	P	0-65								5	10		60-100					Svalbard	Brandner et al. (2017)
Bivalvia	Myida	*Mya truncata*	P	0-65								5	10		90					Svalbard	Brandner et al. (2017)
Bivalvia	Cardiida	*Serripes groenlandicus*	P	0-65								6	7							Kara Sea	Fetzer & Arntz (2008)
Annelida	Polychaeta	*Amphar ete arctica*	B	0-65																Kara Sea	Fetzer & Arntz (2008)
Annelida	Polychaeta	*Artacama proboscidea*	P	6-200								4	6							Kara Sea	Fetzer & Arntz (2008)
Annelida	Polychaeta	*Chone duneri*	P	6-200								6	10							Kara Sea	Fetzer & Arntz (2008)
Annelida	Polychaeta	*Eteone barbata*	P	6-200								3	5							Kara Sea	Fetzer & Arntz (2008)
Annelida	Polychaeta	*Gattyana cf. cirrosa*	P	6-200								5	8							Kara Sea	Fetzer & Arntz (2008)
Annelida	Polychaeta	*Nereis zonata*	B	6-200																Kara Sea	Fetzer & Arntz (2008)
Annelida	Polychaeta	*Nicomache lumbricalis*	B	6-200																Kara Sea	Fetzer & Arntz (2008)

Annelida	Polychaeta	*Pholoe minuta*	P	6-200								6	8							Kara Sea	Fetzer & Arntz (2008)
Annelida	Polychaeta	*Phyllodoce groenlandica*	P	6-200								6	8							Kara Sea	Fetzer & Arntz (2008)
Annelida	Polychaeta	*Polydora quadrilobata*	P	6-200								3	5							Kara Sea	Fetzer & Arntz (2008)
Annelida	Polychaeta	*Prionospio cirrifera*	P	6-200								7	8							Kara Sea	Fetzer & Arntz (2008)
Annelida	Polychaeta	*Scoloplos armiger*	P	6-200								2	5							Kara Sea	Fetzer & Arntz (2008)
Annelida	Polychaeta	*Sphaerodorum flavum*	B	6-200																Kara Sea	Fetzer & Arntz (2008)
Annelida	Polychaeta	*Terebellides stroemi*	B	6-200																Kara Sea	Fetzer & Arntz (2008)
Mollusca		*Macoma calcarea*	P	6-200								5	8							Kara Sea	Fetzer & Arntz (2008)
Echinodermata	Holothuroidea	*Eupyrgus scaber*	P	6-200								5	8							Kara Sea	Fetzer & Arntz (2008)
Echinodermata	Holothuroidea	*Myriotrochus eurycyclus*	P	6-200								5	8							Kara Sea	Fetzer & Arntz (2008)
Echinodermata	Holothuroidea	*Myriotrochus rinki*	P	6-200								5	8							Kara Sea	Fetzer & Arntz (2008)
Echinodermata	Ophiuroidea	*Ophioctenen sericeum*	P	6-200								1	12							Kara Sea	Fetzer & Arntz (2008)
Polychaeta		*Harmothoe sarsi*	P	6-200								6	8							Kara Sea	Fetzer & Arntz (2008)
Polychaeta		*Nereis diversicolor*	P	6-200								3	8							Kara Sea	Fetzer & Arntz (2008)
Polychaeta		*Nereis pelagica*	P	6-200								4	8							Kara Sea	Fetzer & Arntz (2008)

Polychaeta		*Polydora coeca*	P	6-200								5	6							Kara Sea	Fetzer & Arntz (2008)
Polychaeta		*Prionospio malmgreni*	P	6-200								6	8							Kara Sea	Fetzer & Arntz (2008)
Crustacea		*Balanus sp.*	P	6-200								2	8							Kara Sea	Fetzer & Arntz (2008)
Bryozoa		*Group*	P	6	100							6	7							Svalbard	Kuklinski et al. (2013)
Crustacea	Cirripedia	*Group*	P	6	100							6	8	7						Svalbard	Kuklinski et al. (2013)
Mollusca	Bivalvia	*Group*	P	6	100							5	9	7						Svalbard	Kuklinski et al. (2013)
Mollusca	Gastropoda	*Group*	P	6	100							7	10	8						Svalbard	Kuklinski et al. (2013)
Annelida	Polychaeta	*Group*	P	6	100							3	6	5						Svalbard	Kuklinski et al. (2013)
Annelida	Polychaeta	*Spionidae*	P	6	100							4	6	6						Svalbard	Kuklinski et al. (2013)
Echinodermata		*Group*	P	6	100							8	8	8						Svalbard	Kuklinski et al. (2013)
Crustacea	Decapoda	*Paralithodes camtschaticus*	p	0-180								2	4	3						North Norway	Michelsen et al. (2017)
Crustacea	Decapoda	*Hyas sp.*	P	0-180								5	6							North Norway	Michelsen et al. (2017)
Crustacea	Decapoda	*Pagurus pubescens*	P	0-180								6	6							North Norway	Michelsen et al. (2017)
Crustacea	Decapoda	*Pagurus bernhardus*	P	0-180								8	8							North Norway	Michelsen et al. (2017)
Crustacea	Decapoda	*Munida rugosa*	P	0-180								8	8							North Norway	Michelsen et al. (2017)
Crustacea	Cirripedia	*Balanus crenatus*	P	0-180								4	4							North Norway	Michelsen et al. (2017)
Crustacea	Cirripedia	*nauplii*	P	0-180								6	8							North Norway	Michelsen et al. (2017)
Crustacea	Cirripedia	*Balanus sp.*	P	0-180								4	4							North Norway	Michelsen et al. (2017)

Annelida	Polychaeta	*Spionidae*	P	0-180								4	6							North Norway	Michelsen et al. (2017)
Annelida	Polychaeta	*Laonice cirrata*	P	0-180								3	3							North Norway	Michelsen et al. (2017)
Annelida	Polychaeta	*Dipolydora sp.*	P	0-180								4	4							North Norway	Michelsen et al. (2017)
Annelida	Polychaeta	*Scolelepis sp.*	P	0-180								4	5							North Norway	Michelsen et al. (2017)
Annelida	Polychaeta	*Phyllodoce sp.*	P	0-180								5	8							North Norway	Michelsen et al. (2017)
Annelida	Polychaeta	*Owenidae*	P	0-180								5	6							North Norway	Michelsen et al. (2017)
Annelida	Polychaeta	*Pectinaria sp.*	P	0-180								5	5							North Norway	Michelsen et al. (2017)
Annelida	Polychaeta	*Harmothoe sp.*	P	0-180								5	5							North Norway	Michelsen et al. (2017)
Echinodermata	Ophiuroidea	*Ophiuoridea pluteus*	P	0-180								5	8							North Norway	Michelsen et al. (2017)
Echinodermata	Echinoidea	*Echinoidea pluteus*	P	0-180								5	5							North Norway	Michelsen et al. (2017)
Echinodermata	Holothuroidea	*Holothuroidea pentacula*	P	0-180								6	6							North Norway	Michelsen et al. (2017)
Mollusca	Gastropoda	*Prosobranchia veliger*	P	0-180								8	8							North Norway	Michelsen et al. (2017)
Mollusca	Bivalvia	*Bivalvia veliger*	P	0-180								8	8							North Norway	Michelsen et al. (2017)
Mollusca	Bivalvia	*Anomia sp.*	P	0-180								8	8							North Norway	Michelsen et al. (2017)
Bryozoa		*Bryozoa cyphonautes*	P	0-180								8	8							North Norway	Michelsen et al. (2017)
Bryozoa		*Electra pilosa*	P	0-180								6	6							North Norway	Michelsen et al. (2017)
Bryozoa		*Membranipora membranacea*	P	0-180								10	10							North Norway	Michelsen et al. (2017)

Chordata	Ascidiacea	*Ascidiacea larvae*	P	0-180								4	8							North Norway	Michelsen et al. (2017)
Chordata	Appendicularia	*Appendicularia*	P	0-180								5	8							North Norway	Michelsen et al. (2017)
Mollusca	Bivalvia	*Bivalvia veliger*	P	0-250	10	80	10					5	6							Barents Sea	Schlüter & Rachor (2001)
Crustacea	Decapoda	*Galathea spp.*	P	0-100								6	8							Nothwest Norway	Silberberger et al. (2016)
Crustacea	Cirripedia	*Verruca stroemia*	P	0-100								6	8							Nothwest Norway	Silberberger et al. (2016)
Crustacea	Cirripedia	*Balanus balanus*	P	0-100								3	5							Nothwest Norway	Silberberger et al. (2016)
Crustacea	Cirripedia	*Semibalanus balanoides*	P	0-100								3	5							Nothwest Norway	Silberberger et al. (2016)
Bryozoa		*Membranipora membranacea*	P	0-100								5	8							Nothwest Norway	Silberberger et al. (2016)
Annelida	Polychaeta	*Amphinomidae*	P	0-100								6	8							Nothwest Norway	Silberberger et al. (2016)
Annelida	Polychaeta	*Chaetopteridae*	P	0-100								6	8							Nothwest Norway	Silberberger et al. (2016)
Annelida	Polychaeta	*Spionidae*	P	0-100								3	5							Nothwest Norway	Silberberger et al. (2016)
Mollusca	Bivalvia	*Hiatella sp.*	P	0-100								6	8							Nothwest Norway	Silberberger et al. (2016)
Mollusca	Bivalvia	*Mya sp.*	P	0-100								6	8							Nothwest Norway	Silberberger et al. (2016)
Mollusca	Bivalvia	*Mytilidae*	P	0-100								6	8							Nothwest Norway	Silberberger et al. (2016)

Mollusca	Bivalvia	*Anomiidae*	P	0-100								6	8							Nothwest Norway	Silberberger et al. (2016)
Mollusca	Gastropoda	*Littorinidae*	P	0-100								4	8							Nothwest Norway	Silberberger et al. (2016)
Echinodermata	Ophiuroidea	*Ophiuoridea pluteus*	P	0-100								4	6							Nothwest Norway	Silberberger et al. (2016)
Echinodermata	Echinoidea	*Echinoidea pluteus*	P	0-100								4	7							Nothwest Norway	Silberberger et al. (2016)
Mollusca	Bivalvia	*Bivalvia veliger*	P	0-25								5	8							Svalbard	Stübner et al. (2016)
Crustacea	Cirripedia	*Nauplii*	P	0-25								4	6							Svalbard	Stübner et al. (2016)
Annelida	Polychaeta	*Polychaeta larvae*	P	0-25								4	7							Svalbard	Stübner et al. (2016)
Echinodermata		*Ecinodermata larvae*	P	0-25								5	10							Svalbard	Stübner et al. (2016)
Bryozoa		*Bryozoa larvae*	P	0-25								1	3							Svalbard	Stübner et al. (2016)
Crustacea	Decapoda	*Decapoda larvae*	P	0-25								4	8							Svalbard	Stübner et al. (2016)
Crustacea	Euphausiacea	*Euphausiacea larvae*	P	0-110	10	70	20					5	7					63		Southwest Greenland	Teglhus et al. (2015)
General model			P															100		Modelled	O'Connor et al. (2007)

PAME SECRETARIAT
Borgir, v. Nordurslod
Akureyri - Iceland
Tel: +354 461 1355
pame@pame.is
pame.is